



Original research

Development of a sensitive trial-ready poly(GP) CSF biomarker assay for *C9orf72*-associated frontotemporal dementia and amyotrophic lateral sclerosis

Katherine M Wilson,^{1,2} Eszter Katona,^{1,2} Idoia Glaria,^{1,2} Mireia Carcolé ,^{1,2} Imogen J Swift,^{1,3} Aitana Sogorb-Esteve,^{1,3} Carolin Heller ,^{1,3} Arabella Bouzigues,³ Amanda J Heslegrave,¹ Ashvini Keshavan,³ Kathryn Knowles,^{1,3} Saurabh Patil,⁴ Susovan Mohapatra,⁴ Yuanjing Liu,⁴ Jaya Goyal,⁴ Raquel Sanchez-Valle,⁵ Robert Jr Laforce,⁶ Matthias Synofzik ,^{7,8} James B Rowe ,⁹ Elizabeth Finger ,¹⁰ Rik Vandenberghe,^{11,12,13} Christopher R Butler,^{14,15} Alexander Gerhard ,^{16,17} John C Van Swieten ,¹⁸ Harro Seelaar ,¹⁸ Barbara Borroni ,¹⁹ Daniela Galimberti ,^{20,21} Alexandre de Mendonça,²² Mario Masellis,²³ M Carmela Tartaglia,^{24,25} Markus Otto,²⁶ Caroline Graff,^{27,28} Simon Ducharme ,^{29,30} Jonathan M Schott ,³ Andrea Malaspina,^{31,32} Henrik Zetterberg ,^{1,33} Ramakrishna Boyanapalli,⁴ Jonathan D Rohrer ,^{1,3} Adrian M Isaacs ,^{1,2,32} on behalf of the Genetic FTD Initiative (GENFI)

► Additional supplemental material is published online only. To view, please visit the journal online (<http://dx.doi.org/10.1136/jnnp-2021-328710>).

For numbered affiliations see end of article.

Correspondence to

Dr Adrian M Isaacs, UK Dementia Research Institute at UCL, UCL Queen Square Institute of Neurology, London, UK; a.isaacs@ucl.ac.uk

KMW and EK contributed equally.

RB, JDR and AMI are joint senior authors.

Received 21 December 2021
Accepted 4 March 2022



© Author(s) (or their employer(s)) 2022. Re-use permitted under CC BY. Published by BMJ.

To cite: Wilson KM, Katona E, Glaria I, et al. *J Neurol Neurosurg Psychiatry* Epub ahead of print: [please include Day Month Year]. doi:10.1136/jnnp-2021-328710

ABSTRACT

Objective A GGGGCC repeat expansion in the *C9orf72* gene is the most common cause of genetic frontotemporal dementia (FTD) and amyotrophic lateral sclerosis (ALS). As potential therapies targeting the repeat expansion are now entering clinical trials, sensitive biomarker assays of target engagement are urgently required. Our objective was to develop such an assay.

Methods We used the single molecule array (Simoa) platform to develop an immunoassay for measuring poly(GP) dipeptide repeat proteins (DPRs) generated by the *C9orf72* repeat expansion in cerebrospinal fluid (CSF) of people with *C9orf72*-associated FTD/ALS.

Results and conclusions We show the assay to be highly sensitive and robust, passing extensive qualification criteria including low intraplate and interplate variability, a high precision and accuracy in measuring both calibrators and samples, dilutional parallelism, tolerance to sample and standard freeze-thaw and no haemoglobin interference. We used this assay to measure poly(GP) in CSF samples collected through the Genetic FTD Initiative (N=40 *C9orf72* and 15 controls). We found it had 100% specificity and 100% sensitivity and a large window for detecting target engagement, as the *C9orf72* CSF sample with the lowest poly(GP) signal had eightfold higher signal than controls and on average values from *C9orf72* samples were 38-fold higher than controls, which all fell below the lower limit of quantification of the assay. These data indicate that a Simoa-based poly(GP) DPR assay is suitable for use in clinical trials to determine target engagement of therapeutics aimed at reducing *C9orf72* repeat-containing transcripts.

Key messages

- Accurate measurement of dipeptide repeat proteins (DPRs) generated by the frontotemporal dementia and amyotrophic lateral sclerosis-causing repeat expansion in *C9orf72* will be a key tool for assessing target engagement of repeat/DPR lowering strategies in clinical trials.
- Immunoassays have been developed that can detect the poly(GP) DPR in patient cerebrospinal fluid (CSF), but as some patients' poly(GP) levels are close to background, enhanced sensitivity may be needed.
- We report the development of an ultrasensitive CSF poly(GP) detection assay that is fit-for-purpose for clinical trials. This should allow target engagement to be assessed in the vast majority of trial participants, including those with low poly(GP) levels.

INTRODUCTION

A GGGGCC repeat expansion in the first intron of *C9orf72* is the most common genetic cause of both amyotrophic lateral sclerosis (ALS) and frontotemporal dementia (FTD), accounting for 38% and 25% of familial cases, respectively.¹ Healthy individuals most commonly have two repeats,² while people with a *C9orf72* repeat expansion (C9FTD/ALS) can carry hundreds to thousands of repeats.^{3–6} The repeats are transcribed in both sense and antisense direction, leading to the formation of RNA aggregates termed RNA foci.^{7–10} In

addition, repeat-associated non-ATG translation of the repeat expansion leads to the production of dipeptide repeat proteins (DPRs). Translation occurs in all three frames from both sense and antisense transcripts producing five different dipeptide species, poly(GA), poly(GP), poly(GR), poly(PR) and poly(PA). Therapies targeting the *C9orf72* repeat expansion such as small molecules,^{11 12} antisense oligonucleotides (ASOs),^{10 13–18} siRNAs,¹⁹ microRNAs²⁰ and CRISPR-based approaches^{21–23} are rapidly being developed. ASOs targeting the repeat expansion or *C9orf72* transcripts have been shown to reduce both RNA foci and DPR levels in human iPSC-neurons^{13 14 17} and *C9orf72* mouse models.^{10 15–18} In order to progress therapies from the bench to the bedside, biomarkers of disease that reflect target engagement are needed. An important breakthrough was the discovery that poly(GP) can be detected in the cerebrospinal fluid (CSF) of people with C9FTD/ALS using Meso Scale Discovery (MSD) immunoassays, indicating its potential as a target engagement biomarker.^{17 24} Levels of poly(GP) in CSF were not found to correlate with clinical disease markers or neurofilament CSF levels, a non-disease specific biomarker of neurodegeneration.^{17 24} Encouragingly, ASO treatment of mouse models has been shown to lead to durable, decreased poly(GP) levels both in brain tissues and mouse CSF, and a recent study showed reduction in CSF poly(GP) levels in a person with *C9orf72* ALS, showing that CSF poly(GP) levels could be used as a pharmacodynamic biomarker.^{16–18 25}

The single molecule array (Simoa) platform measures immuno-complexes bound to microscopic beads that are isolated in arrays of microwells, large enough for a single bead. Using digital detection the Simoa platform enables single molecule detection.²⁶ As poly(GP) is the most straightforward DPR to measure in CSF, we developed a sensitive, qualified poly(GP) assay using Simoa technology. Following extensive assay development and qualification we measured poly(GP) levels in CSF collected through the Genetic FTD Initiative (GENFI). In this cohort the assay had 100% sensitivity and 100% specificity and showed an eight-fold difference in signal between controls and the patient with C9FTD with the lowest poly(GP) levels, indicating that it can be used as a target engagement biomarker for *C9orf72* FTD/ALS.

MATERIALS AND METHODS
GENFI participants

Fifty-five participants were recruited from GENFI, a natural history study of genetic FTD based across 27 sites in Europe and Canada.²⁷ Participants included 15 symptomatic *C9orf72* expansion carriers (14 with behavioural variant FTD (bvFTD) and 1 with ALS), 25 presymptomatic *C9orf72* expansion carriers and 15 non-carrier relatives, as controls. Pathogenic *C9orf72* expansion length was defined as more than 30 repeats identified by repeat-primed PCR. Participants consisted of 23 men and 32 women, with a mean (SD) age of 49.4 (13.9) years old at sample collection. Within the disease groups: presymptomatic *C9orf72* expansion carriers, 11 men and 14 women, 41.0 (10) years old and symptomatic *C9orf72* expansion carriers, 10 men and 5 women, 64.7 (8.5) years old. Fifteen healthy controls were recruited over the same time period: 2 men and 13 women, 48.2 (11.2) years old. All people in the study underwent a clinical assessment consisting of a medical history with the participant and informant, and physical examination, with symptomatic status diagnosed by a clinician who was an expert in the FTD field.^{28–32} All participants also underwent three-dimensional T1-weighted MRI of the brain. Volumetric measures of whole brain and cortical regions were calculated using a previously

described method that uses the geodesic information flow algorithm, which is based on atlas propagation and label fusion.³³ The study procedures were approved by local ethics committees at each of the participating sites and participants provided informed written consent.

Neurodegenerative disease controls

Twenty participants with Alzheimer’s disease (AD) were recruited from the Wolfson clinical CSF study at University College London (UCL). The cohort consisted of an approximately equal ratio of men to women, an age range of 45–80 years and an AD-like CSF biomarker profile (CSF Aβ42 < 630 pg/mL and CSF total tau/Aβ42 ≥ 0.88)³⁴ previously quantified in clinical routine testing. Twenty participants with non-*C9orf72*-associated FTD were recruited from the Longitudinal Investigation of FTD study at UCL. Eight patients had a diagnosis of bvFTD and 12 were diagnosed with non-fluent variant primary progressive aphasia. All participants had negative genetic testing for FTD-causing mutations. The cohort consisted of 15 men and 5 women, and an age range of 53–79.

CSF and plasma collection

CSF and plasma were collected, processed and stored in aliquots at –80°C according to standardised procedures.³⁵

NfL plasma assay

Plasma neurofilament light chain (NfL) concentration was measured in 8 matched symptomatic *C9orf72* CSF donors, 10 matched presymptomatic CSF donors and 5 matched healthy control CSF donors using the multiplex Neurology 4-Plex A kit (102153, Quanterix, Billerica, Massachusetts) on the Simoa HD-1 Analyzer following manufacturer’s instructions.

Antibodies

Rabbit Polyclonal antibodies ‘GP57’ and ‘GP60’ were produced using a synthetic polypeptide, GP(32) as antigen and provided by Wave Life Sciences. An alternative polyclonal anti-GP antibody ‘GP6834’ was custom-made by Eurogentec, using GP(8) as antigen. The monoclonal poly(GP) antibody TALS 828.179 was obtained from the Developmental Studies Hybridoma Bank, deposited by Target ALS Foundation. Antibody details are summarised in [table 1](#).

Antibody bead conjugation and biotinylation were performed as recommended by Quanterix’s Homebrew Assay Development guide. Briefly, 0.3 mL of carboxylated paramagnetic beads were conjugated with 0.2 mg/mL antibody and 0.3 mg/mL 1-E thyl-3-(3-dimethylaminopropyl) carbodiimide with conjugation performed at 2°C–8°C. This required 80 µg of input antibody. For each biotinylation, 130 µg of antibody was used at 1 mg/mL and a 40:1 ratio of NHS-PEG4-biotin to antibody.

Table 1 Details of polyclonal and monoclonal antibodies tested in single molecule array poly(GP) assays. Rabbit polyclonal antibodies were affinity purified prior to biotinylation and testing

Anti-GP antibody name	Peptide used as antigen	Monoclonal/ polyclonal	Source
GP57	(GP)32	Rabbit polyclonal	Custom made
GP60	(GP)32	Rabbit polyclonal	Custom made
GP6834	(GP)8	Rabbit polyclonal	Custom made
mGP	(GP)8	Mouse monoclonal	TALS 828.179

Assay optimisation

Optimisation of the poly(GP) Simoa assay was performed by testing: two step versus three step assay design, detector antibody concentrations from 0.3 µg/mL to 1.5 µg/mL, streptavidin-β-D-galactosidase (SBG) concentrations from 50 pM to 150 pM, the inclusion of helper beads at different ratios or not at all. Multiple assay combinations were run in parallel to enable selection of optimal conditions. A GST-GP32 standard curve was prepared from two starting stocks (15 000 pg/mL and 1500 pg/mL), serially diluting down from both in diluent A (Quanterix) to create a 9-point standard curve +blank. High (140 pg/mL), middle (75 pg/mL) and low (15 pg/mL) quality control (QC) samples were prepared independently for each assay from a 1500 pg/mL stock of GST-GP32. A positive control human CSF sample from *C9orf72* expansion carriers (QC4) was created by pooling a small volume of CSF from the 40 *C9orf72* expansion carriers in the GENFI cohort.

Curve fitting

To establish best curve fitting we followed a previously described workflow.³⁶ First, heteroscedasticity (the unequal variability of a variable across a range of values of a second variable that predicts it) was assessed by plotting the SD of the average number of enzyme labels per bead (AEB) signals from the calibrators from seven assays, against their concentration (online supplemental figure S1A). As the data showed heteroscedasticity, weighting was determined by plotting log(SD of signals) against log(mean of signals) (online supplemental figure S1B). After applying linear regression and determining the slope value (k), weighting was then calculated using the following formula: $\text{Weighting} = 1/Y^{2k} = 1/Y^{1.9474}$. Curves were recalculated using four parameter logistic (4PL) and five parameter logistic (5PL), with no weighting, 1.9474, or two weighting. Curve fits were assessed using criteria that relative errors (RE) and coefficient of variation (CV) for calibrators were ±15%, and RE and CV for anchor points (1 pg/mL) were ±20%. Curve fitting with 4PL $1/Y^2$ was selected as it led to all calibrator points passing these criteria (online supplemental figure S1C).

Poly(GP) Simoa assay

The optimised Simoa assay (performed on an HD-X instrument, which is an upgraded version of the HD-1 instrument) using TALS 828.179 monoclonal antibody (mGP) beads as capture and a combination of biotinylated GP57 and GP60 (termed GP57*–60*) as detector used the following assay conditions: two-step assay, 0.3 µg/mL detector antibody (GP57*–60*), 50 pM SBG, 150 000 assay beads (mGP) with 350 000 helper beads. CSF was thawed on ice and diluted 1:2 with diluent A (Quanterix). To allow for duplicate measures 250 µL per sample was loaded into the sample plate. Analysts were blind to clinical and genetic status of samples.

Plasma samples were thawed on ice and centrifuged at 14 000 rcf for 15 min at room temperature. 125 µL was then diluted 1:1 with lysate diluent B (Quanterix) to allow duplicate measures per sample. Standard curve was prepared in lysate diluent B diluted 1:2 with control human plasma. Analysts were blind to genetic status of samples.

Statistical analysis

Statistical analysis was carried out using GraphPad Prism software. Data were tested for normality prior to appropriate parametric or non-parametric tests. Mann-Whitney tests were used for comparing two groups, for more than two groups Kruskal-Wallis

tests and Dunn's multiple comparisons test were used. To assess correlations between poly(GP) and clinical features Spearman rho and p (two-tailed) values were calculated.

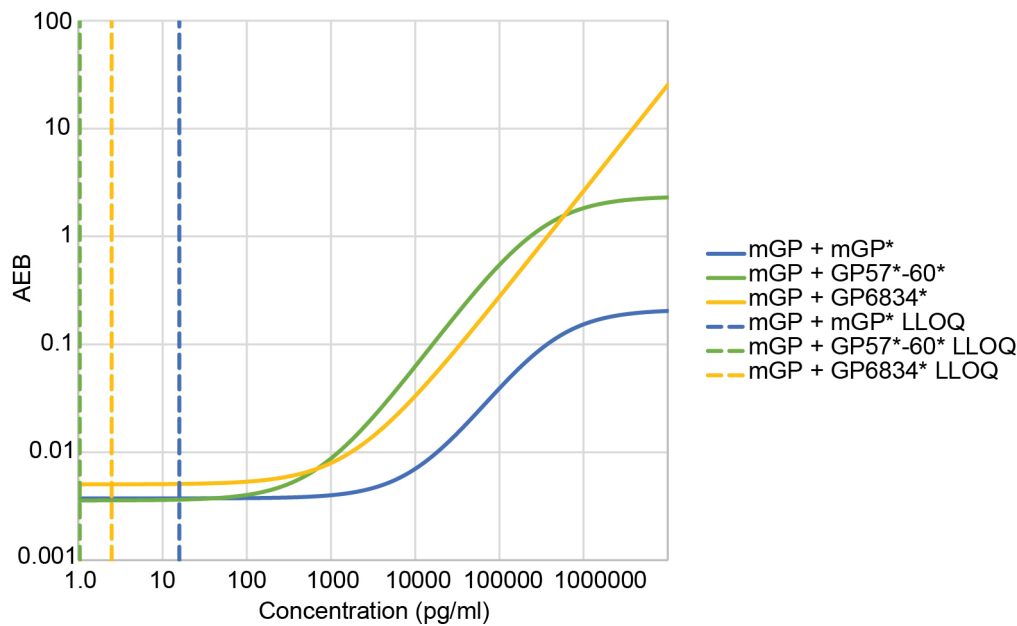
RESULTS

Development of poly(GP) Simoa assay

To develop a sensitive poly(GP) Simoa assay we first optimised assays using the Simoa HD-1 analyser. We tested a mouse monoclonal anti-GP antibody (mGP) and a range of affinity purified rabbit polyclonal antibodies (GP57, GP60 and GP6834) raised against different length GP peptides (table 1). As the long-term goal was to have sufficient antibody quantities for use in a biomarker assay in clinical trials, we combined antibodies GP57 and GP60, which were both raised against a GP32 peptide. We found that using the monoclonal antibody as capture and the combined polyclonal antibodies as detector gave the highest signal to noise ratios for the calibrators and lowest lower limit of quantification (LLOQ) for measurement of a GST-GP32 standard peptide (figure 1). While use of mGP for both capture and detection would have been preferable, due to unlimited supply, even after assay optimisation the mGP +mGP* assay (where * indicates the biotinylated detector antibody) was over 10-fold less sensitive (LLOQ 15.8 pg/mL) than mGP +GP57*–60* (LLOQ 1.04 pg/mL) (figure 1). As mGP +GP57*–60* showed the highest sensitivity, we took this assay forward. To ensure compatibility in the long-term, we next transferred the assay to the newer Simoa HD-X platform. We found the assay required re-optimisation, with the greatest benefit gained from changing the standard curve diluent from lysate diluent B (HD-1) to diluent A (HD-X) (figure 2A). In addition, SBG was lowered from 100 pM to 50 pM for the final HD-X assay, with an LLOQ of 1.17 pg/mL (figure 2B).

Qualification of Simoa poly(GP) assay

To prepare this assay for use in clinical trials it was evaluated using standard biomarker assay qualification criteria (table 2). Precision performance was assessed by analysing standard curves from seven independent assays, performed by two independent researchers. CV was <20% for all standard curve points (figure 3A and online supplemental table S1). Difference from total (DFT) (difference between predicted and actual concentration of calibrators) was below 20% for all calibrators in 6/7 assays (figure 3B and online supplemental table S2). LLOQ was identified as 1 pg/mL with upper limit of quantification at 200 pg/mL. QC samples were prepared by spiking the standard reference material GST-GP32 into diluent A. Upper QC (150 pg/mL), middle QC (75 pg/mL) and lower QC (5 pg/mL) all showed CVs <20% after seven independent runs (figure 3C and online supplemental table S3). DFTs were below 25% for QCs in seven assay runs (figure 3E and online supplemental table S4). Intraplate variability was assessed by measuring three sets of QCs across a plate within a single assay, with CV <5% for all three QCs (figure 3F and online supplemental table S5). An endogenous matrix QC sample (QC4) was generated by pooling human CSF from *C9orf72* expansion positive donors. Poly(GP) concentration of QC4 was measured in four independent assays and the CV was <20% (figure 3G and online supplemental table S7). Intermediate precision was further tested by measurement of QC samples prepared three times. This was repeated by a second analyst (figure 3D and online supplemental table S6). CV was <20% for the sets of QCs prepared independently and between the two analysts.



Antibody pairs	mGP + mGP*	mGP + GP57*-60*	mGP + GP6834*
Upper limit of quantification (ULOQ) (pg/ml)	711	581	1E+100
Lower limit of quantification (LLOQ) (pg/ml)	15.8	1.04	2.28
Signal to noise at LLOQ	2.44	2.51	2.41

Figure 1 Comparison of monoclonal and polyclonal anti-poly(GP) antibodies in Simoa homebrew assays. Homebrew Simoa assay conditions were optimised using different capture antibodies and detector antibodies (*). mGP=monoclonal poly(GP) antibody (TALS 828.179). GP57*-60* is a combination of two custom polyclonal antibodies 'GP57' and 'GP60'. GP6834 is an alternative custom made poly(GP) antibody. Dashed lines show predicted LLOQs for each optimised assay respectively (mGP +mGP*, mGP +GP57*-60*, mGP +GP6834*), calculated using the Quanterix assay developer tool, after running 6-point standard curves using GST-GP32 as standard. AEB, average number of enzyme labels per bead; LLOQ, lower limit of quantification; Simoa, single molecule array.

Dilutional parallelism was assessed by running CSF from six *C9orf72* expansion positive donors either neat, 1:2, 1:4, 1:8 and 1:16 in diluent A. Poly(GP) was detected above background for all dilutions. Using 1:2 as an anchor point the average % error of 4 out of 6 samples had <30% error at 1:4 dilution, passing qualification criteria (figure 3H). The percentage error increased above 30% for the majority of samples at 1:8 and 1:16 (online supplemental table S8 and figure S2). We chose to run samples at 1:2 dilution and recommend further assessment of parallelism within trials with more samples. Freeze-thaw stability of poly(GP) in CSF was tested using QC4 and measuring poly(GP) after 1, 2, and 3 freeze-thaw cycles. The signal and concentration measured had CVs of 4% and 5% respectively indicating no effect of freeze-thaw on detection of endogenous poly(GP) (figure 3G and online supplemental table S9). The freeze-thaw stability of the standard (GST-GP32) was also assessed after 1, 2, or 3 freeze-thaw cycles. Eight of the calibrators passed criteria with CV <20% and DFT <20% (online supplemental table S10). The lowest standard curve point, 1 pg/mL gave a higher DFT after three freeze-thaw cycles, but this is explained by the higher CV in signal measured for the blank in this set of calibrators, and we therefore concluded that it is unlikely that up to three freeze-thaw cycles affects the signal from GST-GP32.

During CSF collection it is possible for blood to contaminate the collected CSF. We tested if haemoglobin interfered with

poly(GP) detection. We spiked a range of haemolysate concentrations (figure 3I) into control CSF and spiked with either 5 pg/mL or 50 pg/mL GST-GP32. 5 pg/mL GST-GP32 spiked in CSF was not affected by any of the haemolysate concentrations tested (online supplemental figure S3). The measurement of 50 pg/mL GST-GP32 spiked in CSF was inhibited (>20%) by addition of 1% haemolysate (figure 3J). At this concentration of haemoglobin, the CSF is visibly red (figure 3I), so samples can be excluded from analysis by appearance if required. Note, none of the CSF samples measured in this study had a red or pink appearance.

Measurement of poly(GP) in CSF from *C9orf72* expansion carriers using the optimised, qualified Simoa assay

We used this sensitive, qualified assay to measure poly(GP) in a cohort of CSF from healthy controls (N=15) and *C9orf72* expansion positive donors (N=40) (demographic details in online supplemental table S11). The assay signal from the lowest *C9orf72* case had signal/noise eightfold over the average signal from control samples, showing a clear separation from signals of control CSF (figure 4A). On average the signal to noise of *C9orf72* cases versus controls was 38-fold. Poly(GP) in CSF from healthy donors was below detection level for 13 out of 15 samples or below LLOQ of the assay for the remaining 2 out of 15 cases. As

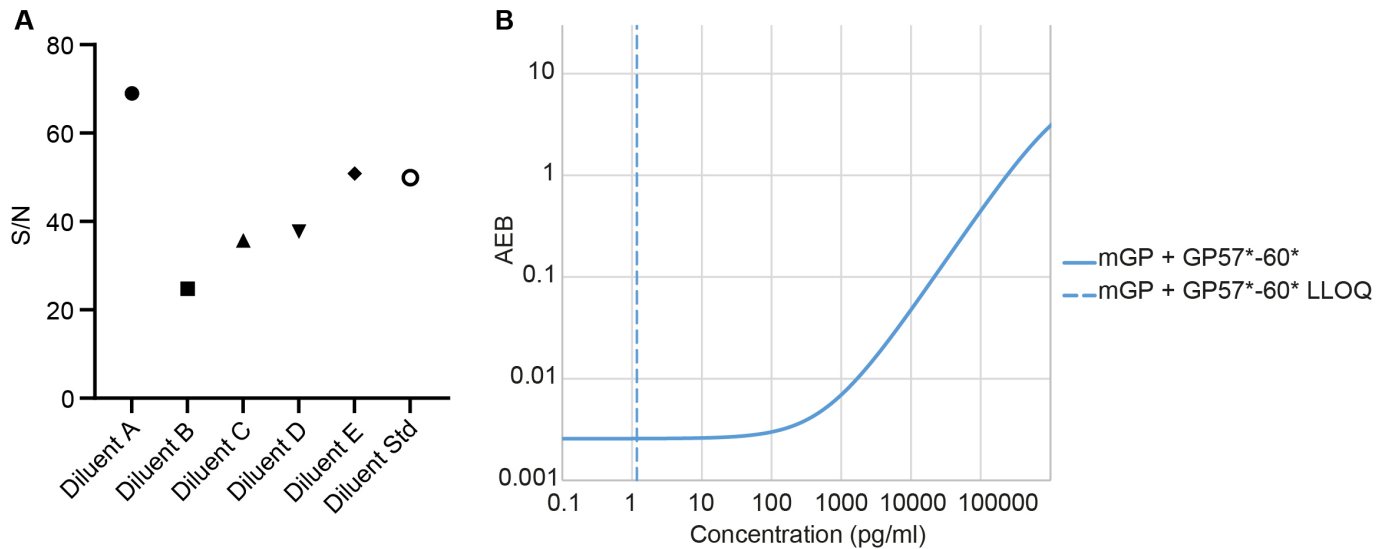


Figure 2 Transfer of poly(GP) assay onto Simoa HD-X. (A) Effect of sample diluents was assessed by comparing signal/noise (S/N) using control human CSF spiked with 25 pg/mL GST-GP32 standard, diluted 1 in 2 with different Quanterix diluents. Samples were run in duplicate on a single two-step Simoa assay (HD-X), using mGP +GP57*–60* Homebrew assay. (B) Standard curve produced from optimised mGP +GP57*–60* HD-X Simoa assay, using GST-GP32 as standard. LLOQ at 1.17 pg/mL shown by dashed line, calculated using the Quanterix assay developer tool. AEB, average number of enzyme labels per bead; CSF, cerebrospinal fluid; LLOQ, lower limit of quantification; Simoa, single molecule array.

poly(GP) was detected above LLOQ in all *C9orf72* cases and in no healthy controls, sensitivity and specificity were both 100%. Poly(GP) measures ranged from 6 to 148 pg/mL in *C9orf72* expansion positive donors. Despite the increased sensitivity of this Simoa assay, the levels of poly(GP) were not statistically different between presymptomatic and symptomatic *C9orf72* expansion positive donors (symptomatic mean=35.2 pg/mL, presymptomatic mean=21.2 pg/mL, $p=0.1348$ Mann-Whitney test), although we observed the same trend observed by others towards higher levels in symptomatic cases^{17 24 37} (figure 4B). We found no difference in poly(GP) levels between male and female

C9orf72 expansion positive donors (online supplemental figure S4A). We found no correlation between CSF poly(GP) levels and age of onset of symptomatic *C9orf72* expansion positive donors ($n=15$) (figure 4C). Interestingly there was a significant, moderate positive correlation ($r=0.3643$) between age at donation and poly(GP) measured in CSF, analysing all 40 *C9orf72* expansion positive cases (figure 4D). However, if the case with the highest poly(GP) level is removed from analysis the p value changes to $p=0.0522$.

Further disease control CSF samples (Alzheimer's disease, $n=20$; non-*C9orf72* FTD, $n=20$) (online supplemental table

Table 2 Biomarker assay qualification criteria for poly(GP) single molecule array assay. Coefficient of variation (CV)=(SD / mean)×100. Difference from Total (DFT)=difference from predicted concentration of calibrators (pg/mL from actual, as % of actual. Quality control samples (QCs) were prepared using GST-GP32 in diluent A.

Parameter	Criteria	Achieved	Data
Precision and accuracy measuring calibrators	75% of calibrators CV≤20% and 75% of calibrators DFT≤±20%.	1×assay 89%. 6× assays 100% of calibrators CV≤20%. 1×assay 89%. 6×assays 100% of calibrators DFT ≤±20%.	Figure 3A and B. online supplemental table 1 and 2.
Precision and accuracy measuring QC samples	High (140 pg/mL), medium (75 pg/mL) and low (15 pg/mL) QCs CV ≤20% and DFT≤±20%.	6/7 assays all QCs had CV≤20%. 6/7 assays all QCs had DFT≤±20%.	Figure 3C and E. online supplemental table 3 and 4.
Intraplate and interplate reproducibility	Repeat measure of QC samples across multiple plates and positioned across a single plate CV ≤20%. Three sets QC samples prepared independently, in two independent assays by two analysts, CV ≤20% and DFT≤±20%.	100% of repeat measures of QC samples CV ≤20%. 100% of QC sets, prepared by two analysts CV≤20% and DFT≤±20%.	Figure 3D and F. online supplemental table 5 and 6.
Precision measuring matrix control sample	Repeated measures of a positive human <i>C9orf72</i> CSF sample should have CV≤20%.	Raw AEB and predicted GP concentration from four assays CV≤20%.	Figure 3G. online supplemental table 7.
Dilutional parallelism	At least three of diluted samples within the assay's range should have DFT within ±30.0%	Using 1:2 as anchor, 4/6 samples at 1:4 had DFT within ±30.0%	Figure 3H. online supplemental table 8 and figure 1.
Freeze–thaw stability	Freeze–thaw stability of matrix control QC. CV ≤25% and DFT ≤±30%. Freeze–thaw stability of calibrators CV≤20%.	After three Freeze–thaw cycles matrix control QC CV≤25% and DFT≤±30%. After three freeze–thaw cycles of calibrators 100% CV ≤20%.	Figure 3. online supplemental table 8 and 10.
Haemoglobin tolerance	Assay should tolerate low levels of haemoglobin within ±20%.	Assay tolerates 0.2% haemolysate spike with measures within ±20%.	Figure 3I and J. online supplemental figure 2.

AEB, average number of enzyme labels per bead.

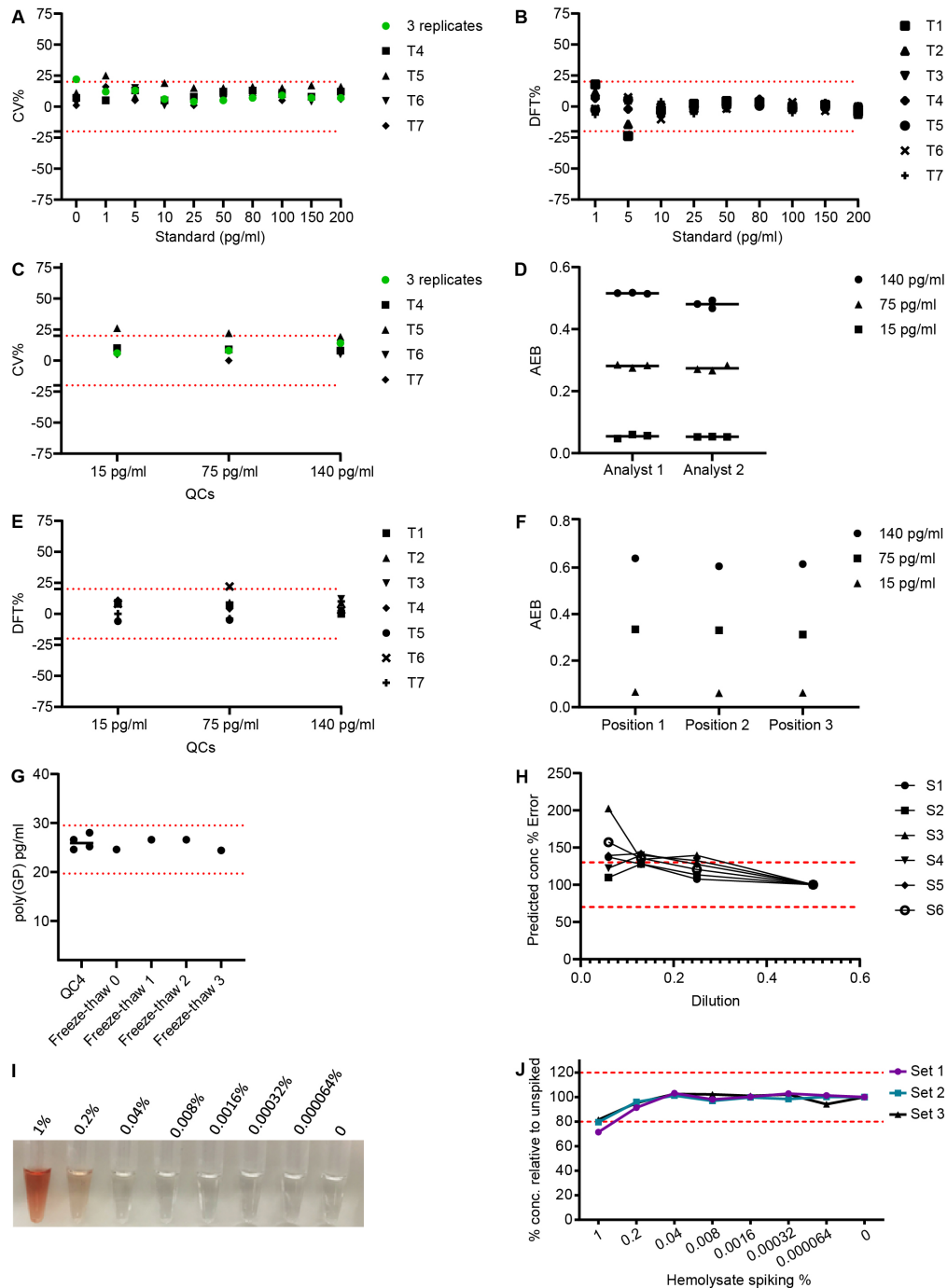


Figure 3 CSF poly(GP) single molecule array (Simoa) assay qualification. Ten point standard curves ranging from 200 to 1 pg/mL and three quality control (QC) samples (15 pg/mL, 75 pg/mL, 140 pg/mL) were prepared using GST-GP32 peptide and measured in seven independent assays. (A) The coefficient of variation (CV) was measured for each standard, calculating first the CV for three initial assays (green dot) and then comparing subsequent assays to the average signal from those three assays. Red dotted line at $\pm 20\%$ acceptance level. (B) The difference from total (DFT) calculated for each standard across seven independent assays. DFT = % difference between predicted concentration and actual concentration of calibrators. Red dotted lines at $\pm 20\%$ acceptance level. (C) CVs for QC samples across seven independent assays. Green dot displaying the CV from the three initial assays. Red dotted lines at $\pm 20\%$ acceptance level. (D) The Simoa assay signal, average number of enzyme labels per bead (AEB), measured for QCs prepared by two different analysts. Each analyst prepared three independent sets of QCs. (E) DFTs calculated for QC samples run in seven independent assays. Red dotted lines at $\pm 20\%$ acceptance level. (F) Intraplate variability assessed by measuring QCs in three different positions across a single assay plate. (G) Human *C9orf72* CSF donor sample (QC4) measured in four independent assays, showing high precision. Furthermore, QC4 underwent 0, 1, 2 or 3 freeze–thaw cycles prior to measurement in a single assay. Red dotted lines at $\pm 20\%$ acceptance level from the fresh measured QC4 sample. (H) Dilutional parallelism measured using six *C9orf72* CSF samples serially diluted, using 1 in 2 dilution as anchor. Predicted concentration % error was calculated comparing the adjusted predicted concentration at each dilution to the concentration of the 1 in 2 diluted sample (set to 100%). Red dotted lines denote $\pm 30\%$ from the expected predicted concentration. (I) Photo of CSF spiked with haemolysate ranging from 1% to 0.000064%. (J) CSF was spiked with haemolysate and serially diluted to give a range of equivalent % haemolysate. CSF was also spiked with 50 pg/mL GST-GP32 and poly(GP) concentration measured using the Simoa assay. Three sets were assayed and % error in predicted concentration was plotted for each sample. Red dotted lines at $\pm 20\%$ from expected poly(GP) concentration.

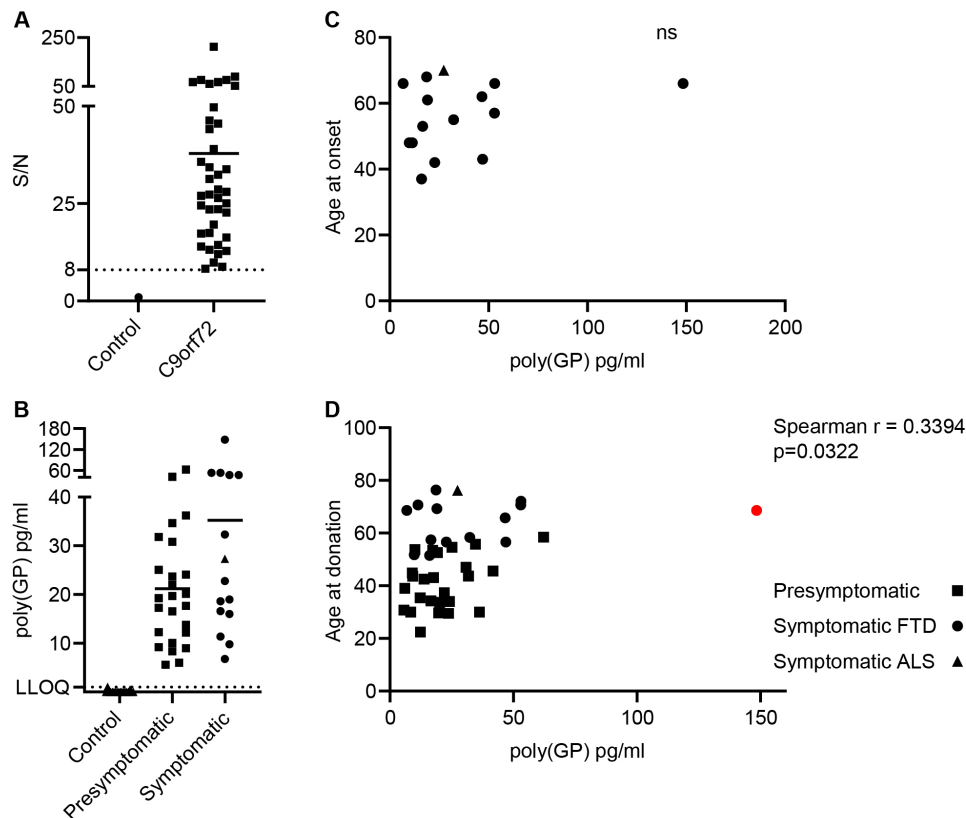


Figure 4 Poly(GP) levels in CSF from *C9orf72* expansion carriers. Poly(GP) levels in CSF from 25 presymptomatic *C9orf72* expansion carriers, 15 symptomatic *C9orf72* carriers and 15 healthy aged matched controls were measured using our optimised Simoa HD-X assay. (A) Signal/noise (S/N) was calculated by dividing the mean AEB signal from duplicate measures of 40 *C9orf72* expansion carriers, by the mean AEB signal of CSF from all 15 healthy controls (plotted here as 1). *C9orf72* expansion carriers had poly(GP) assay signals distinct from healthy controls, with all S/N values above 8. (B) Comparison of poly(GP) levels in presymptomatic and symptomatic *C9orf72* expansion carriers. Fourteen bvFTD cases shown as circles and one ALS case shown as a triangle. Each data point is the average from a duplicate measure from each donor, with bar at mean for each group. Lower limit of quantification (LLOQ) at 1 pg/mL is shown with dotted line, determined by the lowest calibrator tested with acceptable % CV in the assay run. There is no statistical difference in poly(GP) levels between presymptomatic and symptomatic *C9orf72* expansion carriers (Mann-Whitney U test). (C) Age of onset plotted against poly(GP) pg/ml in CSF for 15 symptomatic *C9orf72* expansion carriers. Fourteen bvFTD cases shown as circles and one ALS case shown as a triangle. ns=not significant, no correlation found (Spearman r). (D) Age at donation plotted against CSF poly(GP) levels. Fourteen bvFTD cases shown as circles, one ALS case shown as a triangle and 25 presymptomatic cases shown as squares. Red dot indicates high poly(GP) CSF case, which if removed increases p value to $p=0.0522$. ALS, amyotrophic lateral sclerosis; AEB, average number of enzyme labels per bead; bvFTD, behavioural variant FTD; CSF, cerebrospinal fluid; CV, coefficient of variation; FTD, frontotemporal dementia; Simoa, single molecule array,

S11) were measured using the Simoa poly(GP) assay (online supplemental figure S5). Fresh antibody-coupled beads were prepared for these additional samples and a set of standard calibrators were included to test the performance of the assay run. As expected, all samples were below the LLOQ (online supplemental figure S5).

Where data were available we also tested for correlations between CSF poly(GP) levels and both total brain and lobar volumes. No correlation was found, analysing all *C9orf72* expansion carriers or selecting symptomatic cases only (online supplemental figure S6), consistent with a previous report.³⁷ Plasma NfL is a known biomarker of neurodegeneration. Plasma levels of NfL were measured in 18 of the *C9orf72* expansion carrier CSF donors (including eight symptomatic donors). As expected, plasma NfL levels were significantly higher in symptomatic carriers (online supplemental figure S7A). No correlation was found between CSF poly(GP) and plasma NfL levels analysing the small sample of eight symptomatic cases (online supplemental figure S7B).

We next optimised our poly(GP) Simoa assay for analysis of plasma. Despite the high sensitivity of the Simoa platform we

were unable to detect poly(GP) in plasma from *C9orf72* expansion positive donors. Signals were below LLOQ and there was no difference between control-positive and *C9orf72*-positive signals (online supplemental figure S7C). The two cases of plasma from *C9orf72* expansion carriers which had higher AEB signals were not the same donors with higher than average CSF poly(GP), and there was no correlation between plasma AEB signal and poly(GP) measured in matched CSF samples (online supplemental figure S7D). There is a predicted 200-fold drop in concentration of NfL measured between CSF and plasma. The levels of poly(GP) in CSF were on average 26 pg/mL, so if a similar reduction is observed for poly(GP) a platform capable of detecting in femtogram range maybe required to measure poly(GP) in plasma.

DISCUSSION

We describe the development and qualification of a sensitive Simoa assay for poly(GP) DPRs in CSF. Multiple antibodies were assessed and compared in combinations in a Homebrew Simoa assay, identifying differences in performance across antibody

combinations. In our experience not all polyclonal antibodies behave the same, even when the same peptide sequence was used for antigen. We tested the performance of a monoclonal antibody as both capture and detector in a Homebrew Simoa assay. Unfortunately, the monoclonal antibody tested here did not perform as well as a detector antibody as the polyclonal antibodies, with much higher predicted LLOQs. The reason for this difference is unclear, but the different polyclonal antibodies may recognise different secondary structures of poly(GP).

We used our qualified poly(GP) assay to analyse CSF from a small cohort of CSF samples provided by GENFI, including 15 healthy controls and 40 *C9orf72* expansion carriers. Similar to previously published studies,^{17 24 37} our assay was able to distinguish controls and *C9orf72* expansion carriers. In this cohort we had 100% sensitivity and 100% specificity with poly(GP) measured in CSF from all *C9orf72* expansion carriers, while controls either measured below detection (13/15) or below limit of quantification (2/15), determined at 1 pg/mL. *C9orf72* expansion carriers had a range of poly(GP) from 6 to 148 pg/mL, with all positive sample signals at least eightfold higher than control signals, showing a clear separation of controls from *C9orf72* expansion samples. We did not detect poly(GP) above LLOQ in Alzheimer's disease or patients with non-*C9orf72* FTD. All previous studies used MSD immunoassays and reported the average CSF polyGP signal to be in the low nanogram range,^{17 37} while our assay gives average polyGP levels in the low-medium picogram range. This difference may be attributed to the different calibrators used in the studies, as we have noted that the same antibody can report different concentrations depending on the calibrator used. The use of different calibrators precludes a direct comparison of the different assays. Simoa technology allows detection of single molecules by converting signal from individual beads into a digital output, which we predict will provide higher sensitivity than the MSD assays that rely on an analogue output from each sample well. Although Simoa assays will not be more sensitive than MSD assays in all cases, as this will depend on the specific antibodies used, we do observe higher sensitivity compared with our standard polyGP MSD assay.^{11 38 39} A limitation of our study is that we did not carry out robustness analysis, defined as the capacity of the assay to withstand small but deliberate changes in method parameters such as incubation times, temperatures and buffer pH.⁴⁰

In our cohort of samples we found, similar to previous studies,^{17 24} that compared with presymptomatic carriers, symptomatic carriers had higher levels of poly(GP) comparing mean levels, but this difference was not significant. As we observed a trend towards higher polyGP levels with increasing age at donation, the older age of symptomatic carriers may contribute to this effect, although we note that polyGP levels were shown to remain stable on longitudinal testing over 18–24 months.¹⁷ Meeter *et al*³⁷ found levels in symptomatic carriers were significantly higher.³⁷ This may be due to the larger cohort size tested with more symptomatic donors with higher than average poly(GP) levels included. Within our small cohort there was one symptomatic *C9orf72* carrier with much higher poly(GP) levels than the rest. Age at onset (66 years) and age at donation (68 years) were both within 1 SD from the mean of other symptomatic donors, indicating no effect of higher levels of poly(GP) on these parameters. We did not have repeat length data for this cohort, although given the variability in repeat length between different tissues in the body it would be difficult to interpret repeat length data determined from blood DNA. Lehmer *et al* found no correlation between repeat size and CSF poly(GP) levels in 11 cases where DNA was available.²⁴ Should

postmortem tissue become available from donors in this cohort, it would be interesting to determine repeat length from brain tissue as well as measure propensity of DPR aggregates in the brain to see if poly(GP) CSF levels reflected aggregate burden.

Similar to previous studies we found no correlations between CSF poly(GP) levels and clinical features including; gender, age of onset or brain volume, analysing either total *C9orf72* cases or just symptomatic *C9orf72* carriers.^{17 24 37} We did observe a correlation between CSF poly(GP) levels and age at donation, which is potentially consistent with a relationship between *C9orf72* expansion length and age at DNA sample collection.⁴¹ We analysed NfL levels in a subset of donor matched plasma samples. As expected, symptomatic carriers had higher NfL plasma levels than presymptomatic or controls. As in previous studies that measured NfL in CSF,^{24 37} NfL plasma levels did not correlate with poly(GP) CSF levels. Despite the ability of the Simoa assays to detect at single-molecule levels, we were unable to measure poly(GP) in donor matched plasma samples. Signals for all samples were below quantification and did not correlate with poly(GP) CSF levels. If poly(GP) produced in the brain is present in plasma it will require a more sensitive assay platform and a better understanding of potential matrix effects. In summary, we show utility of the Simoa HD-X platform for detecting poly(GP) in the CSF of people with a *C9orf72* expansion, with assay reliability good enough to be used for target engagement analysis in clinical trials directly targeting *C9orf72* repeat containing transcripts.

Author affiliations

¹UK Dementia Research Institute at UCL, UCL Queen Square Institute of Neurology, London, UK

²Department of Neurodegenerative Disease, UCL Queen Square Institute of Neurology, London, UK

³Dementia Research Centre, Department of Neurodegenerative Disease, UCL Queen Square Institute of Neurology, London, UK

⁴Wave Life Sciences, Cambridge, Massachusetts, USA

⁵Alzheimer's Disease and Other Cognitive Disorders Unit, Neurology Service, Hospital Clínic, Institut d'Investigacions Biomèdiques August Pi I Sunyer, University of Barcelona, Barcelona, Spain

⁶Clinique Interdisciplinaire de Mémoire, Département des Sciences Neurologiques, CHU de Québec, and Faculté de Médecine, Université Laval, Québec City, Québec, Canada

⁷Department of Neurodegenerative Diseases, Hertie-Institute for Clinical Brain Research and Center of Neurology, University of Tübingen, Tübingen, Germany

⁸Center for Neurodegenerative Diseases, (DZNE), Tübingen, Germany

⁹Department of Clinical Neurosciences and Cambridge University Hospitals NHS Trust and Medical Research Council Cognition and Brain Sciences Unit, University of Cambridge, Cambridge, UK

¹⁰Department of Clinical Neurological Sciences, University of Western Ontario, University of Western Ontario, London, Ontario, Canada

¹¹Leuven Brain Institute, KU Leuven, Leuven, Belgium

¹²Laboratory for Cognitive Neurology, Department of Neurosciences, KU Leuven, Leuven, Belgium

¹³Neurology Service, University Hospitals, Leuven, Belgium

¹⁴Nuffield Department of Clinical Neurosciences, Medical Sciences Division, University of Oxford, Oxford, UK

¹⁵Department of Brain Sciences, Imperial College London, London, UK

¹⁶Division of Neuroscience and Experimental Psychology, Wolfson Molecular Imaging Centre, The University of Manchester, Manchester, UK

¹⁷Departments of Geriatric Medicine and Nuclear Medicine, University of Duisburg-Essen, University of Duisburg-Essen, Essen, Germany

¹⁸Department of Neurology, Erasmus Medical Centre, Rotterdam, Netherlands

¹⁹Neurology Unit, Department of Clinical and Experimental Sciences, University of Brescia, Brescia, Italy

²⁰Fondazione IRCCS Ca' Granda, Ospedale Maggiore Policlinico, Milan, Italy

²¹Centro Dino Ferrari, University of Milan, Milan, Italy

²²Faculty of Medicine, University of Lisbon, Lisbon, Portugal

²³Sunnybrook Health Sciences Centre, Sunnybrook Research Institute, University of Toronto, Toronto, Ontario, Canada

²⁴Tanz Centre for Research in Neurodegenerative Disease, University of Toronto, Toronto, Ontario, Canada

²⁵Canadian Sports Concussion Project, Toronto, Ontario, Canada

²⁶Department of Neurology, University of Ulm, Ulm, Germany

²⁷Center for Alzheimer Research, Division of Neurogeriatrics, Department of Neurobiology, Care Sciences and Society, Bioclinicum, Karolinska Institutet, Solna, Sweden

²⁸Unit for Hereditary Dementias, Theme Aging, Karolinska University Hospital, Solna, Sweden

²⁹McConnell Brain Imaging Centre, Montreal Neurological Institute, McGill University, Montreal, Québec, Canada

³⁰Department of Psychiatry, Douglas Mental Health University Institute, McGill University, Montreal, Quebec, Canada

³¹Barts and The London School of Medicine and Dentistry Blizard Institute, London, UK

³²UCL Queen Square Motor Neuron Disease Centre, Department of Neuromuscular Diseases, UCL Queen Square Institute of Neurology, UCL, London, UK

³³Department of Psychiatry and Neurochemistry, Sahlgrenska Academy at the University of Gothenburg, Mölndal, Sweden

Twitter Harro Seelaar @HarroSeelaar, Simon Ducharme @sducharme66, Jonathan M Schott @jmschott and Adrian M Isaacs @isaacs_adrian

Acknowledgements We thank the research participants for their contribution to the study.

Collaborators GENFI consortium: Sónia Afonso (Instituto Ciências Nucleares Aplicadas a Saude, Universidade de Coimbra, Coimbra, Portugal), Maria Rosario Almeida (Faculty of Medicine, University of Coimbra, Coimbra, Portugal), Sarah Anderl-Straub (Department of Neurology, University of Ulm, Ulm, Germany), Christin Andersson (Department of Clinical Neuroscience, Karolinska Institutet, Stockholm, Sweden), Anna Antonell (Alzheimer's disease and Other Cognitive Disorders Unit, Neurology Service, Hospital Clinic, Barcelona, Spain), Silvana Archetti (Biotechnology Laboratory, Department of Diagnostics, ASST Brescia Hospital, Brescia, Italy), Andrea Arighi (Fondazione IRCCS Ca' Granda Ospedale Maggiore Policlinico, Neurodegenerative Diseases Unit, Milan, Italy; University of Milan, Centro Dino Ferrari, Milan, Italy), Mircea Balasa (Alzheimer's disease and Other Cognitive Disorders Unit, Neurology Service, Hospital Clinic, Barcelona, Spain), Myriam Barandiaran (Cognitive Disorders Unit, Department of Neurology, Donostia University Hospital, San Sebastian, Gipuzkoa, Spain; Neuroscience Area, Biodonostia Health Research Institute, San Sebastian, Gipuzkoa, Spain), Nuria Bargalló (Imaging Diagnostic Center, Hospital Clinic, Barcelona, Spain), Robart Bartha (Department of Medical Biophysics, The University of Western Ontario, London, Ontario, Canada; Centre for Functional and Metabolic Mapping, Robarts Research Institute, The University of Western Ontario, London, Ontario, Canada), Benjamin Bender (Department of Diagnostic and Interventional Neuroradiology, University of Tübingen, Tübingen, Germany), Alberto Benussi (Centre for Neurodegenerative Disorders, Department of Clinical and Experimental Sciences, University of Brescia, Italy), Maxime Bertoux (Inserm 1172, Lille, France; CHU, CNR-MAJ, Labex Distalz, LiCEND Lille, France), Anne Bertrand (Sorbonne Université, Paris Brain Institute – Institut du Cerveau – ICM, Inserm U1127, CNRS UMR 7225, AP-HP - Hôpital Pitié-Salpêtrière, Paris, France), Centre pour l'Acquisition et le Traitement des Images, Institut du Cerveau et la Moelle, Paris, France), Valentina Bessi (Department of Neuroscience, Psychology, Drug Research and Child Health, University of Florence, Florence, Italy), Sandra Black (Sunnybrook Health Sciences Centre, Sunnybrook Research Institute, University of Toronto, Toronto, Canada), Martina Bocchetta (Dementia Research Centre, Department of Neurodegenerative Disease, UCL Institute of Neurology, Queen Square, London, UK), Sergi BorregoEcija (Alzheimer's disease and Other Cognitive Disorders Unit, Neurology Service, Hospital Clinic, Barcelona, Spain), Jose Bras (Center for Neurodegenerative Science, Van Andel Institute, Grand Rapids, Michigan, MI 49503, USA), Alexis Brice (Sorbonne Université, Paris Brain Institute – Institut du Cerveau – ICM, Inserm U1127, CNRS UMR 7225, AP-HP - Hôpital Pitié-Salpêtrière, Paris, France), Rose Bruffaerts (Laboratory for Cognitive Neurology, Department of Neurosciences, KU Leuven, Leuven, Belgium; Biomedical Research Institute, Hasselt University, 3500 Hasselt, Belgium), Agnès Camuzat (Alzheimer's disease and Other Cognitive Disorders Unit, Neurology Service, Hospital Clinic, Barcelona, Spain), Marta Cañada (CITA Alzheimer, San Sebastian, Gipuzkoa, Spain), Valentina Cantoni (Centre for Neurodegenerative Disorders, Department of Clinical and Experimental Sciences, University of Brescia, Italy), Paola Caroppo (Fondazione IRCCS Istituto Neurologico Carlo Besta, Milano, Italy), David Cash (Dementia Research Centre, Department of Neurodegenerative Disease, UCL Institute of Neurology, Queen Square, London, UK), Miguel Castelo-Branco (Faculty of Medicine, University of Coimbra, Coimbra, Portugal), Olivier Colliot (Sorbonne Université, Paris Brain Institute – Institut du Cerveau – ICM, Inserm U1127, CNRS UMR 7225, AP-HP - Hôpital Pitié-Salpêtrière, Paris, France; Centre pour l'Acquisition et le Traitement des Images, Institut du Cerveau et la Moelle, Paris, France), Rhian Convery (Centre for Neurodegenerative Disorders, Department of Clinical and Experimental Sciences, University of Brescia, Italy), Thomas Cope (Department of Clinical Neuroscience, University of Cambridge, Cambridge, UK), Adrian Danek (Department of Neurology, Ludwig-Maximilians Universität München, Munich, Germany), Vincent Deramecourt (Inserm 1172, Lille, France; CHU, CNR-MAJ, Labex Distalz, LiCEND Lille, France; Neuroscience Area, Biodonostia Health Research Institute, San Sebastian, Gipuzkoa, Spain), Giuseppe Di Fede (Fondazione IRCCS Istituto Neurologico Carlo Besta, Milano, Italy), Alina Díez (Neuroscience Area, Biodonostia Health Research Institute, San Sebastian, Gipuzkoa, Spain), Diana Duro (Faculty of Medicine, University of Coimbra, Coimbra, Portugal), Chiara Fenoglio (Fondazione IRCCS Ca' Granda Ospedale Maggiore Policlinico, Neurodegenerative Diseases Unit, Milan, Italy; University of Milan, Centro Dino Ferrari, Milan, Italy), Camilla Ferrari (Department of Neuroscience, Psychology, Drug Research and Child Health, University of Florence, Florence, Italy), Catarina B. Ferreira (Laboratory of Neurosciences, Institute of Molecular Medicine, Faculty of Medicine, University of Lisbon, Lisbon, Portugal), Nick Fox (Dementia Research Centre, Department of Neurodegenerative Disease, UCL Institute of Neurology, Queen Square, London, UK), Morris Freedman (Baycrest Health Sciences, Rotman Research Institute, University of Toronto, Toronto, Canada), Giorgio Fumagalli (Fondazione IRCCS Ca' Granda Ospedale Maggiore Policlinico, Neurodegenerative Diseases Unit, Milan, Italy; University of Milan, Centro Dino Ferrari, Milan, Italy), Aurélie Funkiewiez (Sorbonne Université, Paris Brain Institute – Institut du Cerveau – ICM, Inserm U1127, CNRS UMR 7225, AP-HP - Hôpital Pitié-Salpêtrière, Paris, France; Centre de référence des démences rares ou précoces, IM2A, Département de Neurologie, AP-HP - Hôpital Pitié-Salpêtrière, Paris, France), Alazne Gabilondo (Neuroscience Area, Biodonostia Health Research Institute, San Sebastian, Gipuzkoa, Spain), Roberto Gasparotti (Neuroradiology Unit, University of Brescia, Brescia, Italy), Serge Gauthier (Alzheimer Disease Research Unit, McGill Centre for Studies in Aging, Department of Neurology & Neurosurgery, McGill University, Montreal, Québec, Canada), Stefano Gazzina (Neurology, ASST Brescia Hospital, Brescia, Italy), Giorgio Giaccone (Fondazione IRCCS Istituto Neurologico Carlo Besta, Milano, Italy), Ana Gorostidi (Neuroscience Area, Biodonostia Health Research Institute, San Sebastian, Gipuzkoa, Spain), Lisa Graf (Department of Neurodegenerative Diseases, Hertie-Institute for Clinical Brain Research and Center of Neurology, University of Tübingen, Tübingen, Germany), Caroline Greaves (Dementia Research Centre, Department of Neurodegenerative Disease, UCL Institute of Neurology, Queen Square, London, UK), Rita Guerreiro (Center for Neurodegenerative Science, Van Andel Institute, Grand Rapids, Michigan, MI 49503, USA), Tobias Hoegen (Neurologische Klinik, Ludwig-Maximilians-Universität München, Munich, Germany), Begoña Indakoetxea (Cognitive Disorders Unit, Department of Neurology, Donostia University Hospital, San Sebastian, Gipuzkoa, Spain; Neuroscience Area, Biodonostia Health Research Institute, San Sebastian, Gipuzkoa, Spain), Vesna Jelic (Division of Clinical Geriatrics, Karolinska Institutet, Stockholm, Sweden), Lize Jiskoot (Department of Neurology, Erasmus Medical Center, Rotterdam, Netherlands), Ron Keren (The University Health Network, Toronto Rehabilitation Institute, Toronto, Canada), Gregory Kuchinski (Department of Clinical Neuroscience, University of Cambridge, Cambridge, UK; Univ Lille, France; Inserm 1172, Lille, France), Tobias Langheinrich (Division of Neuroscience and Experimental Psychology, Wolfson Molecular Imaging Centre, University of Manchester, Manchester, UK; Manchester Centre for Clinical Neurosciences, Department of Neurology, Salford Royal NHS Foundation Trust, Manchester, UK), Isabelle Le Ber (Sorbonne Université, Paris Brain Institute – Institut du Cerveau – ICM, Inserm U1127, CNRS UMR 7225, AP-HP - Hôpital Pitié-Salpêtrière, Paris, France; Centre de référence des démences rares ou précoces, IM2A, Département de Neurologie, AP-HP - Hôpital Pitié-Salpêtrière, Paris, France; Département de Neurologie, AP-HP - Hôpital Pitié-Salpêtrière, Paris, France), Thibaud Leboviev (Department of Clinical Neuroscience, University of Cambridge, Cambridge, UK; Univ Lille, France; Inserm 1172, Lille, France), Maria João Leitão (Centre of Neurosciences and Cell Biology, Universidade de Coimbra, Coimbra, Portugal), Johannes Levin (Department of Neurology, Ludwig-Maximilians Universität München, Munich, Germany; Department of Neuroscience, Psychology, Drug Research and Child Health, University of Florence, Florence, Italy; Munich Cluster of Systems Neurology (SyNergy), Munich, Germany), Albert Lladó (Alzheimer's disease and Other Cognitive Disorders Unit, Neurology Service, Hospital Clinic, Barcelona, Spain), Gemma Lombardi (Department of Neuroscience, Psychology, Drug Research and Child Health, University of Florence, Florence, Italy), Jolina Lombardi (Department of Neurology, University of Ulm, Ulm, Germany), Sandra Loosli (Neurologische Klinik, Ludwig-Maximilians-Universität München, Munich, Germany), Carolina Maruta (Laboratory of Language Research, Centro de Estudos Egas Moniz, Faculty of Medicine, University of Lisbon, Lisbon, Portugal), Simon Mead (MRC Prion Unit, Department of Neurodegenerative Disease, UCL Institute of Neurology, Queen Square, London, UK), Gabriel Miltenberger (Faculty of Medicine, University of Coimbra, Coimbra, Portugal), Rick van Minkelen (Department of Clinical Genetics, Erasmus Medical Center, Rotterdam, Netherlands), Sara Mitchell (Sunnybrook Health Sciences Centre, Sunnybrook Research Institute, University of Toronto, Toronto, Canada), Fermin Moreno (Cognitive Disorders Unit, Department of Neurology, Donostia University Hospital, San Sebastian, Gipuzkoa, Spain; Neuroscience Area, Biodonostia Health Research Institute, San Sebastian, Gipuzkoa, Spain), Benedetta Nacmias (Department of Neuroscience, Psychology, Drug Research and Child Health, University of Florence, Florence, Italy; IRCCS Fondazione Don Carlo Gnocchi, Florence, Italy), Annabel Nelson (Dementia Research Centre, Department of Neurodegenerative Disease, UCL Institute of Neurology, Queen Square, London, UK), Jennifer Nicholas (Department of Medical Statistics, London School of Hygiene and Tropical Medicine,

London, UK), Linn Öijerstedt (Center for Alzheimer Research, Division of Neurogeriatrics, Department of Neurobiology, Care Sciences and Society, Bioclinicum, Karolinska Institutet, Solna, Sweden); Unit for Hereditary Dementias, Theme Aging, Karolinska University Hospital, Solna, Sweden), Janne M. Papma (Department of Neurology, Erasmus Medical Center, Rotterdam, Netherlands), Florence Pasquier (Inserm 1172, Lille, France; CHU, CNR-MAJ, Labex Distal, LICEND Lille, France), Georgia Peakman (Dementia Research Centre, Department of Neurodegenerative Disease, UCL Institute of Neurology, Queen Square, London, UK), Yolande Pijnenburg (Amsterdam University Medical Centre, Amsterdam VUmc, Amsterdam, Netherlands), Cristina Polito (Department of Biomedical, Experimental and Clinical Sciences "Mario Serio", Nuclear Medicine Unit, University of Florence, Florence, Italy), Enrico Premi (Stroke Unit, ASST Brescia Hospital, Brescia, Italy), Sara Prioni (Fondazione IRCCS Istituto Neurologico Carlo Besta, Milano, Italy), Catharina Prid (Neurologische Klinik, Ludwig-Maximilians-Universität München, Munich, Germany), Veronica Redaelli (Fondazione IRCCS Istituto Neurologico Carlo Besta, Milano, Italy), Daisy Rinaldi (Sorbonne Université, Paris Brain Institute – Institut du Cerveau – ICM, Inserm U1127, CNRS UMR 7225, AP-HP - Hôpital Pitié-Salpêtrière, Paris, France; Centre de référence des démences rares ou précoces, IM2A, Département de Neurologie, AP-HP - Hôpital Pitié-Salpêtrière, Paris, France; Département de Neurologie, AP-HP - Hôpital Pitié-Salpêtrière, Paris, France), Tim Rittman (Department of Clinical Neuroscience, University of Cambridge, Cambridge, UK), Ekaterina Rogava (Tanz Centre for Research in Neurodegenerative Diseases, University of Toronto, Toronto, Canada), Pedro Rosa-Neto (Translational Neuroimaging Laboratory, McGill Centre for Studies in Aging, McGill University, Montreal, Québec, Canada), Giacomina Rossi (Fondazione IRCCS Istituto Neurologico Carlo Besta, Milano, Italy), Martin Rossor (Dementia Research Centre, Department of Neurodegenerative Disease, UCL Institute of Neurology, Queen Square, London, UK), Isabel Santana (University Hospital of Coimbra (HUC), Neurology Service, Faculty of Medicine, University of Coimbra, Coimbra, Portugal; Center for Neuroscience and Cell Biology, Faculty of Medicine, University of Coimbra, Coimbra, Portugal), Beatriz Santiago (Fondazione IRCCS Istituto Neurologico Carlo Besta, Milano, Italy), Dario Saracino (Sorbonne Université, Paris Brain Institute – Institut du Cerveau – ICM, Inserm U1127, CNRS UMR 7225, AP-HP - Hôpital Pitié-Salpêtrière, Paris, France; Centre de référence des démences rares ou précoces, IM2A, Département de Neurologie, AP-HP - Hôpital Pitié-Salpêtrière, Paris, France; Département de Neurologie, AP-HP - Hôpital Pitié-Salpêtrière, Paris, France), Elio Scarpini (Fondazione IRCCS Ca' Granda Ospedale Maggiore Policlinico, Neurodegenerative Diseases Unit, Milan, Italy; University of Milan, Centro Dino Ferrari, Milan, Italy), Sonja Schönecker (Neurologische Klinik, Ludwig-Maximilians-Universität München, Munich, Germany), Rachele Shafei (Dementia Research Centre, Department of Neurodegenerative Disease, UCL Institute of Neurology, Queen Square, London, UK), Christen Shoemith (Department of Clinical Neurological Sciences, University of Western Ontario, London, Ontario, Canada), Sandro Sorbi (Department of Neuroscience, Psychology, Drug Research and Child Health, University of Florence, Florence, Italy; IRCCS Fondazione Don Carlo Gnocchi, Florence, Italy), Miguel Tábuas-Pereira (Neurology Department, Centro Hospitalar e Universitario de Coimbra, Coimbra, Portugal), Fabrizio Tagliavini (Fondazione IRCCS Istituto Neurologico Carlo Besta, Milano, Italy), Mikel Tainta (Neuroscience Area, Biodonostia Health Research Institute, San Sebastian, Gipuzkoa, Spain), Ricardo Taipa (Neuropathology Unit and Department of Neurology, Centro Hospitalar do Porto - Hospital de Santo António, Oporto, Portugal), David Tang-Wai (The University Health Network, Krembil Research Institute, Toronto, Canada), David L Thomas (Neuroimaging Analysis Centre, Department of Brain Repair and Rehabilitation, UCL Institute of Neurology, Queen Square, London, UK), Paul Thompson (Division of Neuroscience and Experimental Psychology, Wolfson Molecular Imaging Centre, University of Manchester, Manchester, UK), Carolyn Timberlake (Department of Clinical Neuroscience, University of Cambridge, Cambridge, UK), Pietro Tiraboschi (Fondazione IRCCS Istituto Neurologico Carlo Besta, Milano, Italy), Emily Todd (Dementia Research Centre, Department of Neurodegenerative Disease, UCL Institute of Neurology, Queen Square, London, UK), Philip Van Damme (Neurology Service, University Hospitals Leuven, Belgium; Laboratory for Neurobiology, VIB-KU Leuven Centre for Brain Research, Leuven, Belgium), Mathieu Vandenbulcke (Geriatric Psychiatry Service, University Hospitals Leuven, Belgium; Neuropsychiatry, Department of Neurosciences, KU Leuven, Leuven, Belgium), Ana Verdelho (Department of Neurosciences and Mental Health, Centro Hospitalar Lisboa Norte - Hospital de Santa Maria & Faculty of Medicine, University of Lisbon, Lisbon, Portugal), Jorge Villanua (OSATEK, University of Donostia, San Sebastian, Gipuzkoa, Spain), Jason Warren (Dementia Research Centre, Department of Neurodegenerative Disease, UCL Institute of Neurology, Queen Square, London, UK), Carlo Wilke (Department of Neurodegenerative Diseases, Hertie-Institute for Clinical Brain Research and Center of Neurology, University of Tübingen, Tübingen, Germany), Elisabeth Wlasich (Neurologische Klinik, Ludwig-Maximilians-Universität München, Munich, Germany), Miren Zulaica (Neuroscience Area, Biodonostia Health Research Institute, San Sebastian, Gipuzkoa, Spain).

Contributors Conceived and designed study: SM, AM, HZ, RB, JDR, AMI. Performed experiments/analysed data: KMW, EK, IG, MC, IS, AS-E, CH, AB, AJH, SP, YL, JG. Provided GENFI samples: RS-V, RJL, MS, JBR, EF, RV, CRB, AG, JCVS, HS, BB, DG, AdM, MM, MCT, MO, CG, SD. Provided disease control samples: AK, KK, JMS, JDR. Wrote

first draft: KMW, EK, JDR, AMI. Reviewed manuscript: All authors. AMI is responsible for the overall content as guarantor.

Funding This work was funded by Wave Life Sciences, the European Research Council (ERC) under the European Union's Horizon 2020 research and innovation programme (648716 - C9ND) (AMI), the UK Dementia Research Institute, which receives its funding from UK DRI, funded by the UK Medical Research Council, Alzheimer's Society and Alzheimer's Research UK. The Dementia Research Centre is supported by Alzheimer's Research UK, Alzheimer's Society, Brain Research UK and The Wolfson Foundation. This work was supported by the NIHR UCL/H Biomedical Research Centre, the Leonard Wolfson Experimental Neurology Centre (LWENC) Clinical Research Facility and the NIHR Cambridge Biomedical Research Centre (BRC-1215-20014). The views expressed are those of the authors and not necessarily those of the NIHR or the Department of Health and Social Care. AK is supported by a Weston Brain Institute and Selfridges Group Foundation award (UB170045). JMS is supported by Engineering and Physical Sciences Research Council (EP/J020990/1), British Heart Foundation (PG/17/90/33415), EU's Horizon 2020 research and innovation programme (666992). HZ is a Wallenberg Scholar. Simoa instruments used were funded by Wellcome Trust, Fidelity International Foundation and UK DRI. JDR is supported by the Miriam Marks Brain Research UK Senior Fellowship and has received funding from an MRC Clinician Scientist Fellowship (MR/M008525/1) and the NIHR Rare Disease Translational Research Collaboration (BRC149/NS/MH). This work was also supported by the MRC UK GENFI grant (MR/M023664/1), the Bluefield Project and the JPND GENFI-PROX grant (2019-02248). Several authors of this publication are members of the European Reference Network for Rare Neurological Diseases - Project ID No 739510.

Competing interests SP, SM, YL, JG and RB were paid employees of Wave Life Sciences during completion of this work. JDR is on a Medical Advisory Board for Wave Life Sciences. JMS has received research funding from Avid Radiopharmaceuticals (a wholly owned subsidiary of Eli Lilly), has consulted for Roche Pharmaceuticals, Biogen, Merck and Eli Lilly, given educational lectures sponsored by GE Healthcare, Eli Lilly, and Biogen, and serves on a Data Safety Monitoring Committee for Axon Neuroscience SE. HZ has served at scientific advisory boards for Alector, Eisai, Denali, Roche Diagnostics, Wave, Samumed, Siemens Healthineers, Pinteon Therapeutics, Nergven, AZTherapies and CogRx, has given lectures in symposia sponsored by Collectricon, Fujirebio, Alzecure and Biogen, and is a co-founder of Brain Biomarker Solutions in Gothenburg AB (BBS), which is a part of the GU Ventures Incubator Program (outside submitted work). JBR has provided consultancy unrelated to the current work for Asceneuron, Astex, Biogen, UCB, SV Health, Curasan.

Patient consent for publication Not applicable.

Ethics approval This study involves human participants and was approved by The NHS Health Research Authority London - Camden & Kings Cross Research Ethics Committee, 16/LO/0465. Participants gave informed consent to participate in the study before taking part.

Provenance and peer review Not commissioned; externally peer reviewed.

Data availability statement Data are available upon reasonable request.

Supplemental material This content has been supplied by the author(s). It has not been vetted by BMJ Publishing Group Limited (BMJ) and may not have been peer-reviewed. Any opinions or recommendations discussed are solely those of the author(s) and are not endorsed by BMJ. BMJ disclaims all liability and responsibility arising from any reliance placed on the content. Where the content includes any translated material, BMJ does not warrant the accuracy and reliability of the translations (including but not limited to local regulations, clinical guidelines, terminology, drug names and drug dosages), and is not responsible for any error and/or omissions arising from translation and adaptation or otherwise.

Open access This is an open access article distributed in accordance with the Creative Commons Attribution 4.0 Unported (CC BY 4.0) license, which permits others to copy, redistribute, remix, transform and build upon this work for any purpose, provided the original work is properly cited, a link to the licence is given, and indication of whether changes were made. See: <https://creativecommons.org/licenses/by/4.0/>.

ORCID iDs

Mireia Carcolé <http://orcid.org/0000-0001-5054-9016>
 Carolin Heller <http://orcid.org/0000-0002-1934-6162>
 Matthis Synofzik <http://orcid.org/0000-0002-2280-7273>
 James B Rowe <http://orcid.org/0000-0001-7216-8679>
 Elizabeth Finger <http://orcid.org/0000-0003-4461-7427>
 Alexander Gerhard <http://orcid.org/0000-0002-8071-6062>
 John C Van Swieten <http://orcid.org/0000-0001-6278-6844>
 Harro Seelaar <http://orcid.org/0000-0003-1989-7527>
 Barbara Borroni <http://orcid.org/0000-0001-9340-9814>
 Daniela Galimberti <http://orcid.org/0000-0002-9284-5953>
 Simon Ducharme <http://orcid.org/0000-0002-7309-1113>

Jonathan M Schott <http://orcid.org/0000-0003-2059-024X>
 Henrik Zetterberg <http://orcid.org/0000-0003-3930-4354>
 Jonathan D Rohrer <http://orcid.org/0000-0002-6155-8417>
 Adrian M Isaacs <http://orcid.org/0000-0002-6820-5534>

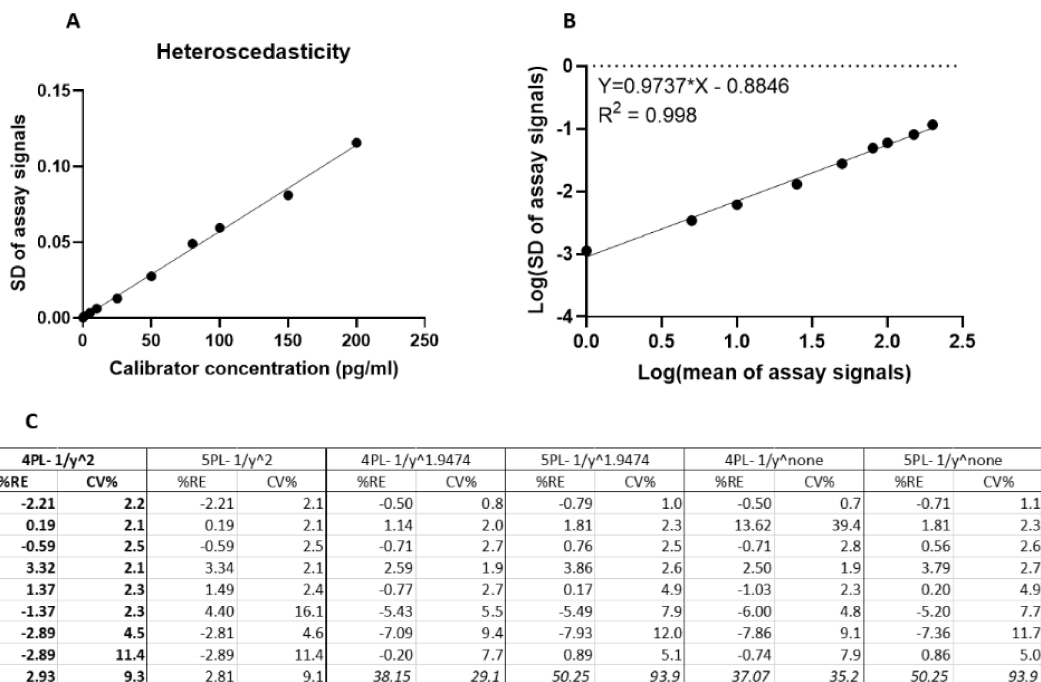
REFERENCES

- Majounie E, Renton AE, Mok K, et al. Frequency of the C9orf72 hexanucleotide repeat expansion in patients with amyotrophic lateral sclerosis and frontotemporal dementia: a cross-sectional study. *Lancet Neurol* 2012;11:323–30.
- Rutherford NJ, Heckman MG, DeJesus-Hernandez M. Length of normal alleles of C9ORF72 GGGGCC repeat do not influence disease phenotype. *Neurobiol Aging* 2012.
- van Blitterswijk M, DeJesus-Hernandez M, Niemantsverdriet E, et al. Association between repeat sizes and clinical and pathological characteristics in carriers of C9orf72 repeat expansions (Xpansize-72): a cross-sectional cohort study. *Lancet Neurol* 2013;12:978–88.
- Beck J, Poulter M, Hensman D, et al. Large C9orf72 hexanucleotide repeat expansions are seen in multiple neurodegenerative syndromes and are more frequent than expected in the UK population. *Am J Hum Genet* 2013;92:345–53.
- Renton AE, Majounie E, Waite A, et al. A hexanucleotide repeat expansion in C9ORF72 is the cause of chromosome 9p21-linked ALS-FTD. *Neuron* 2011;72:257–68.
- DeJesus-Hernandez M, Mackenzie IR, Boeve BF, et al. Expanded GGGGCC hexanucleotide repeat in noncoding region of C9ORF72 causes chromosome 9p-linked FTD and ALS. *Neuron* 2011;72:245–56.
- Mizielinska S, Lashley T, Norona FE, et al. C9orf72 frontotemporal lobar degeneration is characterised by frequent neuronal sense and antisense RNA foci. *Acta Neuropathol* 2013;126:845–57.
- Zu T, Liu Y, Bañez-Coronel M, et al. RAN proteins and RNA foci from antisense transcripts in C9ORF72 ALS and frontotemporal dementia. *Proc Natl Acad Sci U S A* 2013;110:E4968–77.
- Gendron TF, Bieniek KF, Zhang Y-J, et al. Antisense transcripts of the expanded C9ORF72 hexanucleotide repeat form nuclear RNA foci and undergo repeat-associated non-ATG translation in c9FTD/ALS. *Acta Neuropathol* 2013;126:829–44.
- Lagier-Tourenne C, Baughn M, Rigo F, et al. Targeted degradation of sense and antisense C9orf72 RNA foci as therapy for ALS and frontotemporal degeneration. *Proc Natl Acad Sci U S A* 2013;110:E4530–9.
- Simone R, Balendra R, Moens TG, et al. G-quadruplex-binding small molecules ameliorate C9orf72 FTD/ALS pathology *in vitro* and *in vivo*. *EMBO Mol Med* 2018;10:22–31.
- Wang ZF, Ursu A, Childs-Disney JL. The Hairpin Form of r(G 4 C 2) exp in c9ALS/FTD Is Repeat-Associated Non-ATG Translated and a Target for Bioactive Small Molecules. *Cell Chem Biol* 2019.
- Donnelly CJ, Zhang P-W, Pham JT, et al. RNA toxicity from the ALS/FTD C9ORF72 expansion is mitigated by antisense intervention. *Neuron* 2013;80:415–28.
- Sareen D, O'Rourke JG, Meera P, et al. Targeting RNA foci in iPSC-derived motor neurons from ALS patients with a C9orf72 repeat expansion. *Sci Transl Med* 2013;5:ra149.
- O'Rourke JG, Bogdanik L, Muhammad AKMG, et al. C9orf72 BAC transgenic mice display typical pathologic features of ALS/FTD. *Neuron* 2015;88:892–901.
- Jiang J, Zhu Q, Gendron TF, et al. Gain of toxicity from ALS/FTD-linked repeat expansions in C9ORF72 is alleviated by antisense oligonucleotides targeting GGGGCC-Containing RNAs. *Neuron* 2016;90:535–50.
- Gendron TF, Chew J, Stankowski JN, et al. Poly(GP) proteins are a useful pharmacodynamic marker for C9ORF72-associated amyotrophic lateral sclerosis. *Sci Transl Med* 2017;9. doi:10.1126/scitranslmed.aai7866. [Epub ahead of print: 29 03 2017].
- Liu Y, Dodart J-C, Tran H, et al. Variant-selective stereopure oligonucleotides protect against pathologies associated with C9orf72-repeat expansion in preclinical models. *Nat Commun* 2021;12:847.
- Hu J, Rigo F, Prakash TP, et al. Recognition of c9orf72 mutant RNA by single-stranded silencing RNAs. *Nucleic Acid Ther* 2017;27:87–94.
- Martier R, Liefhebber JM, Miniarikova J, et al. Artificial microRNAs targeting C9orf72 can reduce accumulation of Intra-nuclear transcripts in ALS and FTD patients. *Mol Ther Nucleic Acids* 2019;14:593–608.
- Krishnan G, Zhang Y, Gu Y, et al. CRISPR deletion of the C9ORF72 promoter in ALS/FTD patient motor neurons abolishes production of dipeptide repeat proteins and rescues neurodegeneration. *Acta Neuropathol* 2020;140:81–4.
- Pinto BS, Saxena T, Oliveira R, et al. Impeding transcription of expanded microsatellite repeats by deactivated Cas9. *Mol Cell* 2017;68:479–90.
- Batra R, Nelles DA, Pirie E, et al. Elimination of toxic microsatellite repeat expansion RNA by RNA-Targeting Cas9. *Cell* 2017;170:899–912.
- Lehmer C, Oeckl P, Weishaupt JH. Poly-GP in cerebrospinal fluid links C9orf72 - associated dipeptide repeat expression to the asymptomatic phase of ALS / FTD. *EMBO Mol Med* 2017.
- Tran H, Moazami MP, Yang H. Suppression of mutant C9orf72 expression by a potent mixed backbone antisense oligonucleotide. *Nat Med*.
- Rissin DM, Kan CW, Campbell TG, et al. Single-molecule enzyme-linked immunosorbent assay detects serum proteins at subfemtomolar concentrations. *Nat Biotechnol* 2010;28:595–9.
- Rohrer JD, Nicholas JM, Cash DM, et al. Presymptomatic cognitive and neuroanatomical changes in genetic frontotemporal dementia in the genetic frontotemporal dementia initiative (GENFI) study: a cross-sectional analysis. *Lancet Neurol* 2015;14:253–62.
- Rascovsky K, Hodges JR, Knopman D, et al. Sensitivity of revised diagnostic criteria for the behavioural variant of frontotemporal dementia. *Brain* 2011;134:2456–77.
- Gorno-Tempini ML, Hillis AE, Weintraub S, et al. Classification of primary progressive aphasia and its variants. *Neurology* 2011;76:1006–14.
- Brooks BR, Miller RG, Swash M. El Escorial revisited: revised criteria for the diagnosis of amyotrophic lateral sclerosis. *Amyotroph Lateral Scler* 2000.
- Armstrong MJ, Litvan I, Lang AE, et al. Criteria for the diagnosis of corticobasal degeneration. *Neurology* 2013;80:496–503.
- Höglinger GU, Respondek G, Stamelou M. Clinical diagnosis of progressive supranuclear palsy: the movement disorder Society criteria. *Mov Disord* 2017.
- Cardoso MJ, Modat M, Wolz R, et al. Geodesic information flows: Spatially-Variant graphs and their application to segmentation and fusion. *IEEE Trans Med Imaging* 2015;34:1976–88.
- Weston PSJ, Paterson RW, Modat M, et al. Using florbetapir positron emission tomography to explore cerebrospinal fluid cut points and gray zones in small sample sizes. *Alzheimers Dement* 2015;1:440–6.
- Woollacott IOC, Nicholas JM, Heslegrave A, et al. Cerebrospinal fluid soluble TREM2 levels in frontotemporal dementia differ by genetic and pathological subgroup. *Alzheimers Res Ther* 2018;10:1–14. 2018.
- X Y J D, E S, et al. A Simple Approach to Determine a Curve Fitting Model with a Correct Weighting Function for Calibration Curves in Quantitative Ligand Binding Assays. *Aaps J* 2018;20.
- Meeter LHH, Gendron TF, Sias AC. Poly(GP), neurofilament and grey matter deficits in C9orf72 expansion carriers. *Ann Clin Transl Neurol* 2018.
- Moens TG, Mizielinska S, Niccoli T, et al. Sense and antisense RNA are not toxic in Drosophila models of C9orf72-associated ALS/FTD. *Acta Neuropathol* 2018;135:445–57.
- Quaeghebeur A, Glaria I, Lashley T, et al. Soluble and insoluble dipeptide repeat protein measurements in C9orf72-frontotemporal dementia brains show regional differential solubility and correlation of poly-GR with clinical severity. *Acta Neuropathol Commun* 2020;8:184.
- Lee JW, Devanarayan V, Barrett YC, et al. Fit-for-purpose method development and validation for successful biomarker measurement. *Pharm Res* 2006;23:312–28.
- Fournier C, Barbier M, Camuzat A, et al. Relations between C9orf72 expansion size in blood, age at onset, age at collection and transmission across generations in patients and presymptomatic carriers. *Neurobiol Aging* 2019;74:234.e1–234.e8.

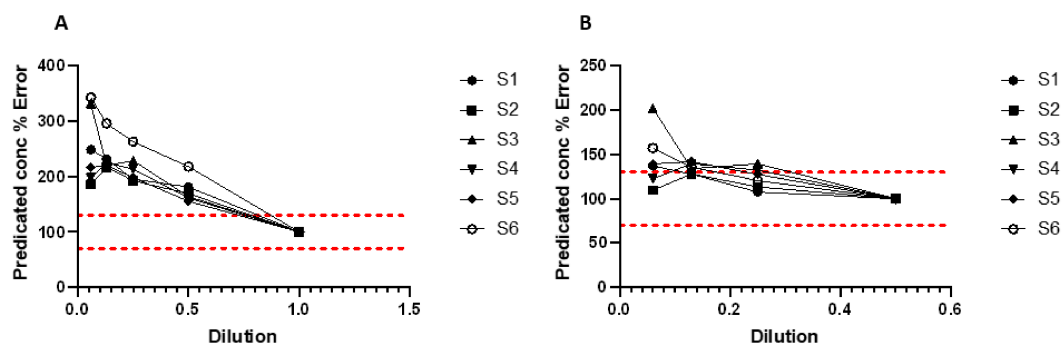
Development of a sensitive trial-ready poly(GP) CSF biomarker assay for *C9orf72*-associated frontotemporal dementia and amyotrophic lateral sclerosis

Katherine M Wilson^{1,2*}, Eszter Katona^{1,2*}, Idoia Glaria^{1,2}, Mireia Carcolé^{1,2}, Imogen J. Swift^{1,3}, Aitana Sogorb-Esteve^{1,3}, Carolin Heller^{1,3}, Arabella Bouzigues¹, Amanda J Heslegrave¹, Ashvini Keshavan³, Kathryn Knowles^{1,3}, Saurabh Patil⁴, Susovan Mohapatra⁴, Yuanjing Liu⁴, Jaya Goyal⁴, Raquel Sanchez-Valle⁵, Robert Laforce⁶, Matthis Synofzik^{7,8}, James B. Rowe⁹, Elizabeth Finger¹⁰, Rik Vandenberghe^{11,12,13}, Christopher R. Butler^{14,15}, Alexander Gerhard^{16,17}, John C. van Swieten¹⁸, Harro Seelaar¹⁸, Barbara Borroni¹⁹, Daniela Galimberti^{20,21}, Alexandre de Mendonça²², Mario Masellis²³, M. Carmela Tartaglia²⁴, Markus Otto²⁵, Caroline Graff^{26,27}, Simon Ducharme^{28,29}, Jonathan M Schott³, Andrea Malaspina^{30,31}, Henrik Zetterberg^{1,32}, Ramakrishna Boyanapalli^{4†}, Jonathan D Rohrer^{1,3†}, Adrian M Isaacs^{1,2‡}, on behalf of the Genetic FTD Initiative (GENFI)^a

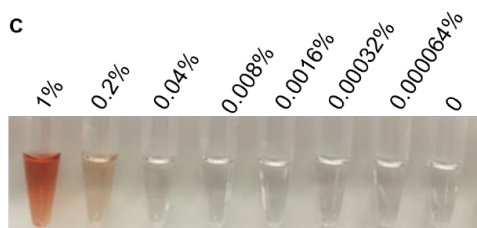
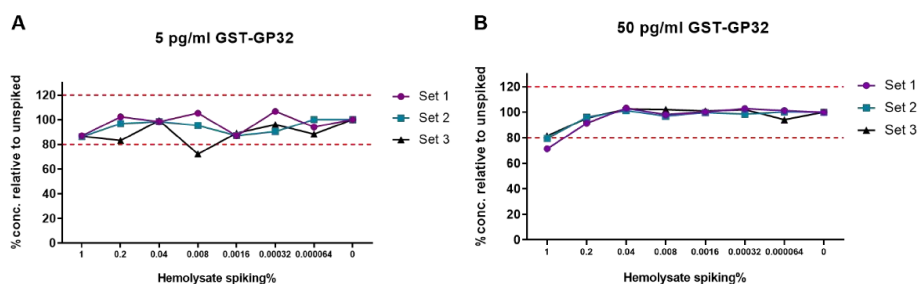
Supplemental Information



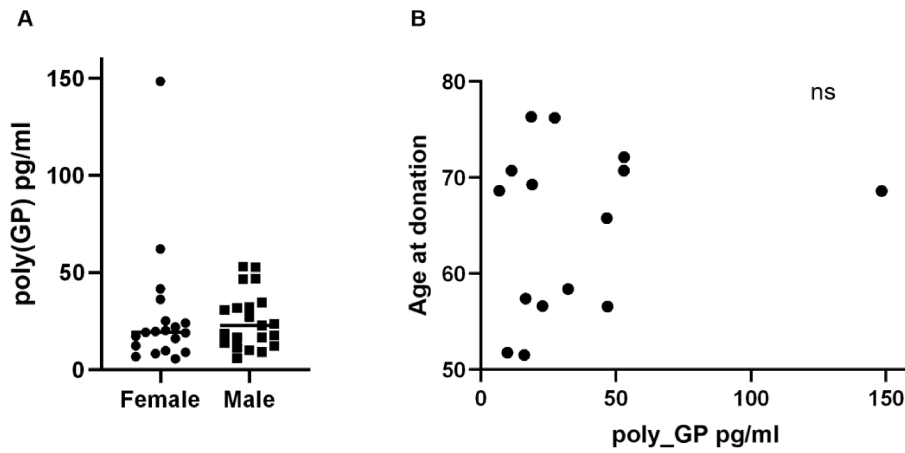
Supplementary figure 1. Assessment of curve fitting. A) Assessment of heteroscedasticity of data carried out by plotting standard deviation of assay signals (AEB) from the calibrator curve standards from 7 independent assays, against the calibrator concentration (pg/ml). B) To calculate weighting, linear regression was applied after plotting Log(standard deviation of assay signals) against Log(mean of assay signals) and the slope of the line (k) used in the formula: weighting= 1/Y^{2k}. C) Curves were recalculated using 4PL and 5PL, with no weighting, 1.9474, or 2 weighting. Curve fits were assessed using criteria that % cumulative relative errors (RE%) and CV% for calibrators were +/- 15%, and RE% and CV% for anchor points (1 pg/ml) were +/- 20%. When 4PL 1/Y² was used for curve fitting, all calibrator points passed these criteria and 4PL 1/Y² was therefore chosen.



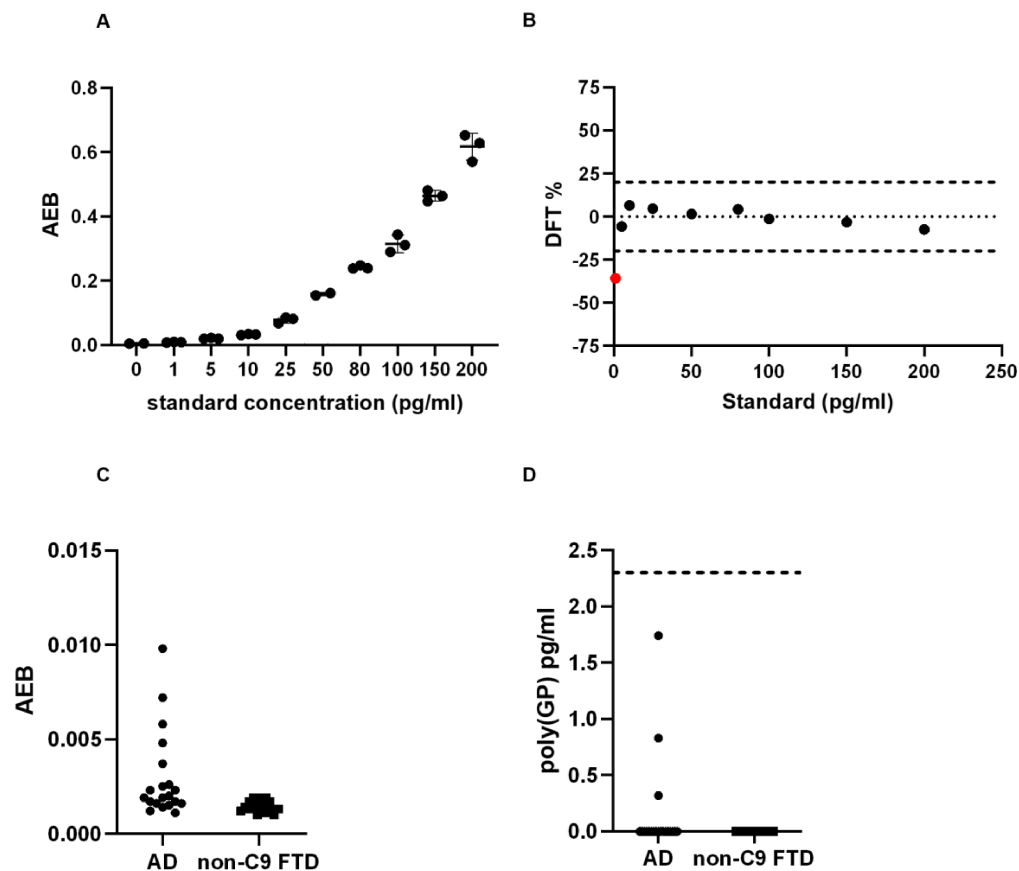
Supplementary figure 2. Dilutional parallelism. CSF from six *C9orf72* expansion positive donors was measured either neat, 1:2, 1:4, 1:8 and 1:16 diluted in diluent A. The mean AEB from duplicate measures was used to predict concentration at each dilution. **A)** The neat sample concentration was used as anchor and the % error was calculated comparing the adjusted predicted concentration at each dilution to the concentration of the neat sample. **B)** The 1:2 diluted sample used as anchor instead. Red dotted lines denote +/- 30% from the expected predicted concentration.



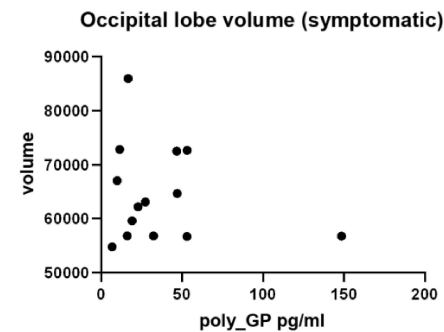
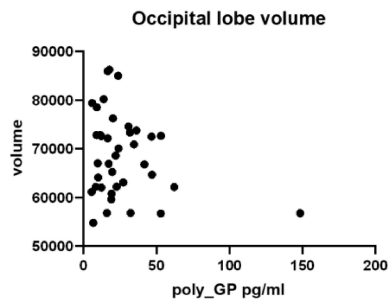
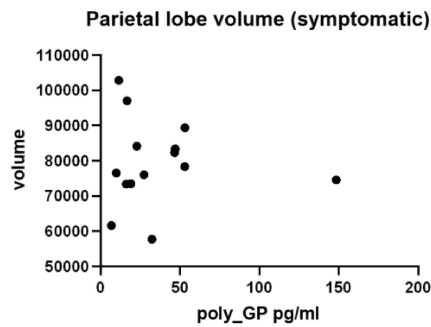
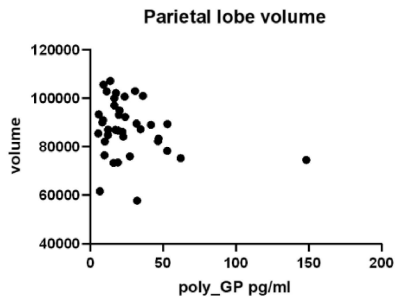
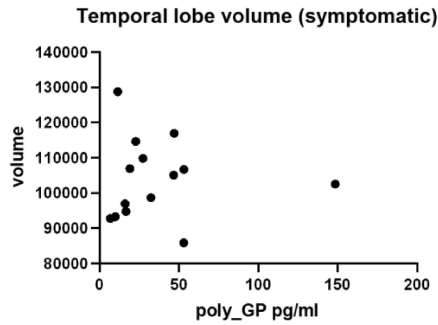
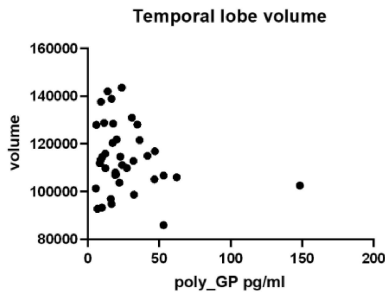
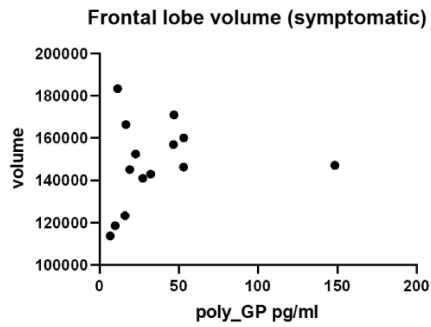
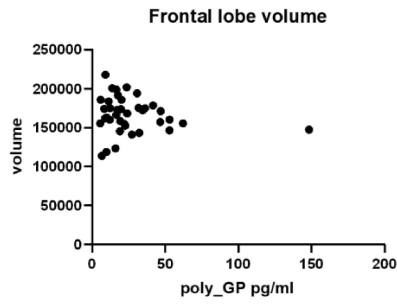
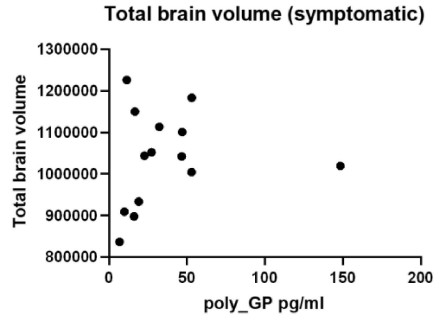
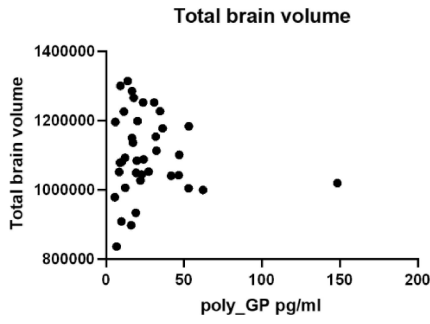
Supplementary figure 3. Haemoglobin interference. Control CSF was spiked with haemolysate and serially diluted to give a range of equivalent % haemolysate. CSF was also spiked with either 5 pg/ml (A) or 50 pg/ml (B) GST-GP32 and poly(GP) concentration measured using Simoa assay. Three sets at each GST-GP32 concentration were assayed and % error in predicted concentration was plotted for each sample. Red dotted lines at +/- 20% from expected poly(GP) concentration. C) Visual appearance of CSF after haemolysate spiking.



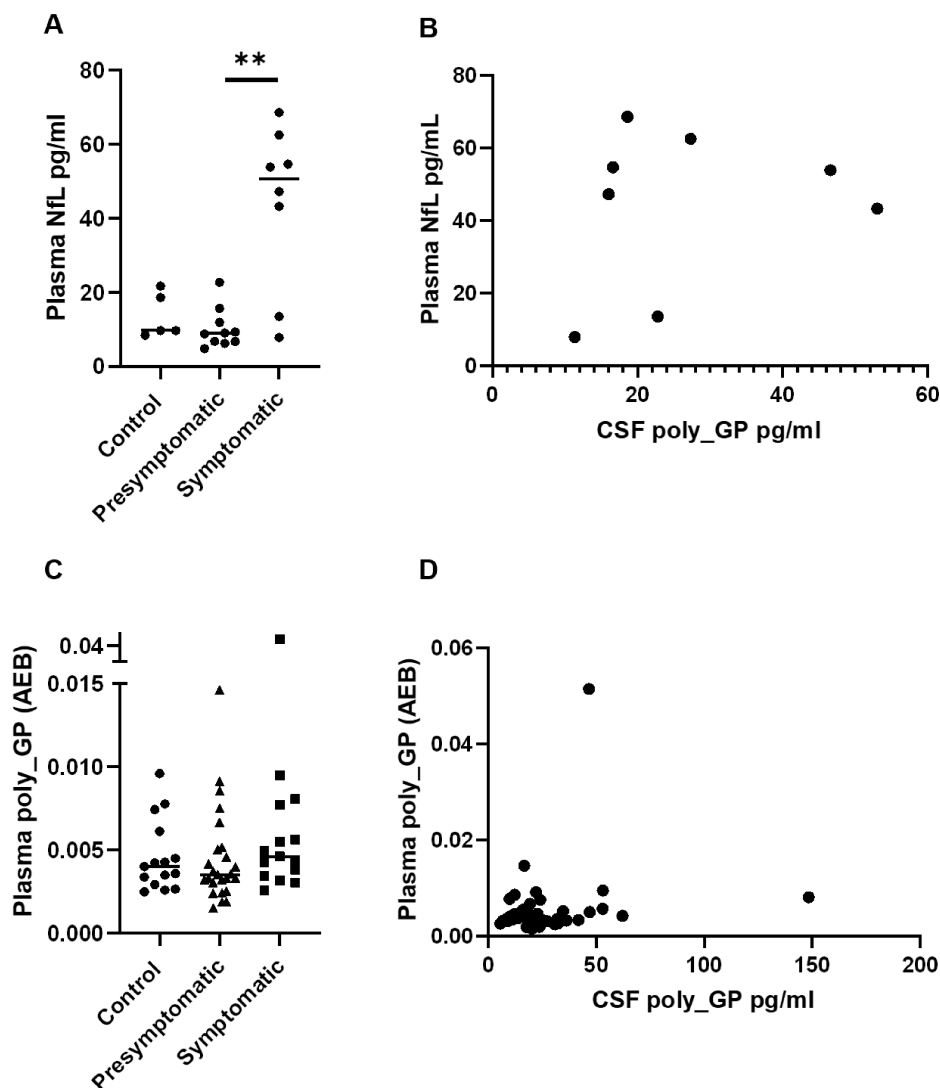
Supplementary Figure 4. Analysis of poly(GP) CSF levels with clinical features. A) No difference between female and male *C9orf72* expansion carriers in CSF poly(GP) levels. **B)** Age at visit for symptomatic *C9orf72* expansion carriers plotted against CSF poly(GP) levels.



Supplementary Figure 5. Assessment of Alzheimer's disease and non-C9orf72 expansion FTD patient CSF. In order to run control neurodegenerative disease patient CSF, additional GP57*-60* antibody was coupled to Simoa beads. Using this newly generated capture reagent, CSF from 20 Alzheimer's disease and 20 non-C9orf72 expansion FTD carriers (12 nonfluent variant primary progressive aphasia and 8 behavioural variant FTD) were assessed for poly(GP) levels. Standard calibrators were run at the same time to assess the assay performance. **A)** AEB values from poly(GP) standards run in triplicate (mean and std). **B)** The difference from total (DFT) calculated for each standard for this assay. DFT = % difference between predicted concentration and actual concentration of calibrators. Dotted lines at +/- 20% acceptance level. The 1 pg/ml standard had a DFT of -36%. **C)** Raw AEB values for each sample, each dot represents the mean of duplicate measures. **D)** Predicted poly(GP) pg/ml values for each sample based on the standard calibrators used for this assay. 37/40 samples had AEB values too low to quantify. The dotted line (at 2.3 pg/ml) is the LLOQ predicted for this assay using the Quanterix assay developer tool.



Supplementary Figure 6. Analysis of brain volume with poly(GP) CSF levels. Left-hand side; total brain volume, temporal lobe, parietal lobe, occipital lobe and frontal lobe volumes against poly(GP) CSF levels from *C9orf72* expansion carriers (N=38). Right-hand side analysis of same regions from symptomatic *C9orf72* expansion carriers (N=14).



Supplementary Figure 7. Analysis of plasma biomarkers from matched CSF donors. Plasma samples from 5 controls, 10 presymptomatic and 8 symptomatic *C9orf72* expansion carriers who also had poly(GP) CSF measured. **A)** Plasma NfL levels were significantly higher in symptomatic carriers compared to presymptomatic carriers (Kruskal Wallis and Dunn's multiple comparisons, ** $p < 0.01$). **B)** No correlation was observed between plasma NfL levels and CSF poly(GP) levels in the available matched samples from 8 symptomatic cases. **C)** Raw AEB signals from Simoa assay optimised to measure poly(GP) in plasma. No difference was observed between controls or *C9orf72* expansion carriers. **D)** Raw AEB signals from plasma samples plotted against matched samples CSF poly(GP) levels.

	Avg. from 3 independent assays		Comp. TEST4 to average		Comp. TEST5 to average		Comp. TEST6 to average		Comp. TEST7 to average	
Calibration curve	Analyst 1		Analyst 2		Analyst 2		Analyst 1		Analyst 2	
pg/ml	Mean AEB	CV%	AEB	CV% comp.	AEB	CV% comp.	AEB	CV% comp.	AEB	CV% comp.
200	0.8360	7%	0.7042	12%	1.0470	16%	0.7481	8%	0.7647	6%
150	0.6185	7%	0.5497	8%	0.7831	17%	0.5882	4%	0.5689	6%
100	0.4337	9%	0.3752	10%	0.5382	15%	0.3729	11%	0.4064	5%
80	0.3400	7%	0.2831	13%	0.4256	16%	0.3012	9%	0.3000	9%
50	0.2182	5%	0.1848	12%	0.2682	15%	0.2003	6%	0.1957	8%
25	0.1117	4%	0.0992	8%	0.1381	15%	0.1009	7%	0.1101	1%
10	0.0453	6%	0.0421	5%	0.0597	19%	0.0458	1%	0.0432	3%
5	0.0255	13%	0.0212	13%	0.0287	8%	0.0205	15%	0.0236	5%
1	0.0058	12%	0.0054	5%	0.0083	25%	0.0062	5%	0.0073	16%
0	0.0022	22%	0.0020	7%	0.0026	11%	0.0021	3%	0.0023	1%

Calibration curve	Test 1	Test 2	Test 3	Test 4	Test 5	Test 6	Test 7
pg/ml	DFT %	DFT %	DFT %	DFT %	DFT %	DFT %	DFT %
200	-4.48	-6.03	-1.56	-1.07	-0.32	-0.05	-1.85
150	1.44	2.77	1.23	-2.12	0.82	-3.53	0.38
100	-0.95	0.16	0.34	-1.35	-1.23	3.40	-5.00
80	3.60	4.65	0.91	5.86	0.51	3.15	4.57
50	4.43	1.58	-1.30	3.23	0.78	-1.78	2.67
25	2.17	-1.64	-0.12	-2.33	-0.33	-0.48	-5.80
10	-2.88	1.03	-0.78	-5.98	-4.75	-10.31	3.83
5	-23.87	-14.18	4.63	-2.05	5.25	7.46	2.53
1	17.80	11.03	-3.91	6.68	-2.64	-1.79	-6.40
0	NaN	NaN	NaN	NaN	NaN	NaN	NaN

Supplementary table 1 and 2) Standard curve CV% and DFT% assessment.

CV% calculated from average AEB values from 3 initial standard curves. Total of 7 assays carried out by 2 independent analysts. DFT = difference from total % predicted concentration of standards (pg/ml) versus actual.

QCs	Mean for 3 set of QCs on		Comp. TEST4 to average		Comp. TEST5 to average		Comp. TEST6 to average		Comp. TEST7 to average	
	Mean AEB	CV%	Mean AEB	CV% comp.	Mean AEB	CV% comp.	Mean AEB	CV% comp.	Mean AEB	CV% comp.
HQC 140pg/ml	0.5540	14%	0.4940	8%	0.7309	19%	0.5160	5%	0.4856	9%
MQC 75pg/ml	0.3066	8%	0.2714	9%	0.4197	22%	0.2752	8%	0.3062	0%
LQC 15pg/ml	0.0610	6%	0.0526	10%	0.0888	26%	0.0568	5%	0.0651	5%

Supplementary table 3) Assessment of quality control samples (QCs) CV%.

QCs	Test 1	Test 2	Test 3	Test 4	Test 5	Test 6	Test 7
	DFT %	DFT %	DFT %	DFT %	DFT %	DFT %	DFT %
HQC 140pg/ml	0%	9%	12%	3%	1%	3%	10%
MQC 75pg/ml	7%	9%	6%	4%	-5%	22%	-4%
LQC 15pg/ml	8%	10%	9%	11%	-6%	8%	0%

Supplementary table 4) Assessment of quality control samples (QCs) DFT%.

Intraplate variability	Position 1		Position 2		Position 3		Average of 3 sets	
	Mean AEB	CV%	Mean AEB	CV%	Mean AEB	CV%	Mean AEB	Total CV%
HQC 140pg/ml	0.6394	6%	0.6058	1%	0.6149	2%	0.6201	3%
MQC 75pg/ml	0.3342	2%	0.3305	0%	0.3125	2%	0.3257	4%
LQC 15pg/ml	0.0651	1%	0.0605	3%	0.0618	1%	0.0625	4%

Supplementary table 5) Intraplate variability assessment of CV%.

Preparation variability	Analyst 1								Analyst 2								Total Mean		Total CV	
	Prep. 1		Prep. 2		Prep. 3		Assay Mean		Prep. 1		Prep. 2		Prep. 3		Assay Mean					
QCs	Mean AEB	CV%	Mean AEB	CV%	Mean AEB	CV%	Mean AEB	CV%	Mean AEB	CV%	Mean AEB	CV%	Mean AEB	CV%	Mean AEB	CV%	Mean AEB	CV%		
HQC 140pg/ml	0.5160	1%	0.5140	3%	0.5180	2%	0.5160	0%	0.4940	1%	0.4814	2%	0.4675	2%	0.4930	2%	0.4985	4%		
MQC 75pg/ml	0.2752	NaN	0.2835	3%	0.2852	9%	0.2813	2%	0.2714	1%	0.2831	2%	0.2666	6%	0.2876	0%	0.2775	3%		
LQC 15pg/ml	0.0568	3%	NaN	14%	0.0604	2%	0.0586	4%	0.0526	3%	0.0540	12%	0.0526	5%	0.0594	11%	0.0553	6%		

Supplementary table 6) Reproducibility assessment using independently prepared QCs.

Matrix control: QC4	Test 1	Test 2	Test 3	Test 4	CV%
Mean AEB	0.0526	0.0576	0.0696	0.0553	13%
Predicted concentration pg/ml	26.7	28.1	24.6	25.2	6%

Supplementary table 7) Reproducibility of matrix control CV%.

	neat - ancore	1:2			1:4			1:8			1:16		
	Mean conc.	Mean conc.	Predicted neat	Error%	Mean conc.	Predicted neat	Error%	Mean conc.	Predicted neat	Error%	Mean conc.	Predicted neat	Error%
S1	15.16	13.76	27.5	-82%	7.40	29.6	-95%	4.39	35.2	-132%	2.36	37.7	-149%
S2	11.75	9.96	19.9	-70%	5.66	22.6	-92%	3.19	25.5	-117%	1.37	21.8	-86%
S3	11.68	9.58	19.2	-64%	6.68	26.7	-129%	3.21	25.7	-120%	1.59	38.8	-232%
S4	21.84	17.63	35.3	-61%	11.68	46.7	-114%	6.16	49.3	-126%	2.70	43.2	-98%
S5	11.68	9.08	18.2	-55%	5.78	23.1	-98%	3.22	25.8	-121%	1.03	25.3	-117%
S6	8.62	9.41	18.8	-118%	5.67	22.7	-163%	3.19	25.5	-196%	1.21	29.6	-243%
Average:				-75%			-115%			-135%			-154%
	1:2 - ancore	1:4			1:8			1:16					
	Mean conc.	Mean conc.	Predicted 1:2	Error%	Mean conc.	Predicted 1:2	Error%	Mean conc.	Predicted 1:2	Error%			
S1	13.76	7.40	14.8	7%	4.39	17.6	-28%	2.36	18.9	-37%			
S2	9.96	5.66	11.3	-14%	3.19	12.8	-28%	1.37	10.9	-10%			
S3	9.58	6.68	13.4	-39%	3.21	12.8	-34%	1.59	19.4	-102%			
S4	17.63	11.68	23.4	-32%	6.16	24.6	-40%	2.70	21.6	-22%			
S5	9.08	5.78	11.6	-27%	3.22	12.9	-42%	1.03	12.6	-39%			
S6	9.41	5.67	11.3	-21%	3.19	12.8	-36%	1.21	14.8	-57%			
Average:				-21%			-35%			-45%			

Supplementary table 8) Dilutional parallelism was assessed by running CSF from six C9orf72 expansion positive donors either neat, 1:2, 1:4, 1:8 and 1:16 in diluent A.

QC4	Meas. 1	Meas. 2	Mean AEB	CV%	Pred. conc. (pg/ml)	CV% for mean AEB	CV% for pred. conc (pg/ml)
Fresh	0.0737	0.0654	0.0696	8%	24.6	4%	5%
Freeze-thaw 1	0.0805	0.0691	0.0748	11%	26.5		
Freeze-thaw 2	0.0732	0.0769	0.0751	4%	26.6		
Freeze-thaw 3	0.0698	0.0685	0.0691	1%	24.4		

Supplementary table 9) Freeze-thaw stability of poly(GP) from human CSF.

pg/ml	Mean AEB				CV% fresh	CV% fresh	CV% fresh	% Error in prediction concentration			
	Fresh	Freeze-thaw 1	Freeze-thaw 2	Freeze-thaw 3	vs. F-T 1	vs. F-T 2	vs. F-T 3	Fresh	Freeze-thaw 1	Freeze-thaw 2	Freeze-thaw 3
200	0.7481	0.7675	0.7258	0.7303	2%	2%	2%	-0.05	-1.22	-3.51	-11.97
150	0.5882	0.5773	0.5568	0.5373	1%	4%	6%	-3.53	1.43	-0.01	-3.75
100	0.3729	0.3964	0.3822	0.3662	4%	2%	1%	3.40	1.42	2.00	-0.74
80	0.3012	0.3280	0.3003	0.3001	6%	0%	0%	3.15	-0.75	5.55	-1.05
50	0.2003	0.2067	0.2086	0.1846	2%	3%	6%	-1.78	0.89	-3.28	4.52
25	0.1009	0.1167	0.1004	0.0978	10%	0%	2%	-0.48	-9.09	1.52	2.87
10	0.0458	0.0426	0.0456	0.0375	5%	0%	14%	-10.31	5.27	-11.82	12.17
5	0.0205	0.0231	0.0200	0.0215	8%	2%	3%	7.46	2.23	4.53	3.90
1	0.0062	0.0064	0.0054	0.0072	2%	10%	10%	-1.79	-3.95	2.52	-34.34
0	0.0021	0.0018	0.0020	0.0013	14%	4%	33%	NaN	NaN	NaN	NaN

Supplementary table 10) Freeze-thaw stability of GST-GP32 standard.

	Controls	Alzheimer's disease	Non-C9orf72 FTD	C9orf72 Expansion Carriers	
				Presymptomatic	Symptomatic
N	15	20	20	26	17
Age at CSF	48.2 (11.2)	61.2 (5.6)	65.6 (8.9)	40.3 (10.5)	64.1 (8.2)
Sex (% female)	86.7	45	25.0	57.7	41.2
MMSE (/30)	29.1 (1.5)	20.0 (5.5)	24.2 (5.0)	29.7 (0.8)	22.8 (6.3)

Supplementary Table 11) Demographics of cases used in the study. *N*, number of participants. Values are shown as mean (standard deviation).

Appendix

List of GENFI consortium authors:



Sónia Afonso¹, Maria Rosario Almeida², Sarah Anderl-Straub³, Christin Andersson⁴, Anna Antonell⁵, Silvana Archetti⁶, Andrea Arighi⁷, Mircea Balasa⁸, Myriam Barandiaran⁹, Nuria Bargalló¹⁰, Robart Bartha¹¹, Benjamin Bender¹², Alberto Benussi¹³, Maxime Bertoux^{14,15}, Anne Bertrand^{16,17}, Valentina Bessi¹⁹, Sandra Black²⁰, Martina Bocchetta²¹, Sergi Borrego-Ecija⁸, Jose Bras²², Alexis Brice¹⁶, Rose Bruffaerts^{23,24}, Agnès Camuzat⁸, Marta Cañada²⁵, Valentina Cantoni¹³, Paola Caroppo²⁶, David Cash²¹, Miguel Castelo-Branco², Olivier Colliot^{16,17}, Rhian Convery¹³, Thomas Cope²⁷, Adrian Danek¹⁸, Vincent Deramecourt^{29,30,31}, Giuseppe Di Fede²⁶, Alina Díez³¹, Diana Duro², Chiara Fenoglio⁷, Camilla Ferrari³², Catarina B. Ferreira³³, Nick Fox²¹, Morris Freedman³⁴, Giorgio Fumagalli⁷, Aurélie Funkiewiez^{16,35}, Alazne Gabilondo³¹, Roberto Gasparotti³⁷, Serge Gauthier³⁸, Stefano Gazzina³⁹, Giorgio Giaccone²⁶, Ana Gorostidi³⁶, Lisa Graf⁴⁰, Caroline Greaves²¹, Rita Guerreiro²², Tobias Hoegen⁴¹, Begoña Indakoetxea⁹, Vesna Jelic⁴², Lize Jiskoot⁴³, Ron Keren⁴⁴, Gregory Kuchcinski^{27,28,29}, Tobias Langheinrich^{45,46}, Isabelle Le Ber^{16,35,47}, Thibaud Lebouvier^{27,28,29}, Maria João Leitão⁴⁸, Johannes Levin^{18,19,50}, Albert Lladó⁸, Gemma Lombardi³², Jolina Lombardi³, Sandra Loosli⁵¹, Carolina Maruta⁵², Simon Mead⁵³, Gabriel Miltenberger², Rick van Minkelen⁵⁴, Sara Mitchell²⁰, Fermin Moreno⁹, Benedetta Nacmias^{32,55}, Annabel Nelson²¹, Jennifer Nicholas⁵⁶, Linn Öijerstedt^{57,58}, Janne M. Pappa⁴³, Florence Pasquier^{14,15}, Georgia Peakman²¹, Yolande Pijnenburg⁵⁹, Cristina Polito⁶⁰, Enrico Premi⁶¹, Sara Prioni²⁶, Catharina Prix⁵¹, Veronica Redaelli²⁶, Daisy Rinaldi^{16,35,47}, Tim Rittman²⁷, Ekaterina Rogaeva⁶², Pedro Rosa-Neto⁶³, Giacomina Rossi²⁶, Martin Rossor²¹, Isabel Santana⁶⁴, Beatriz Santiago²⁶, Dario Saracino^{16,35,47}, Elio Scarpini⁷, Sonja Schönecker⁵¹, Rachelle Shafei²¹, Christen Shoemaker⁶⁵, Sandro Sorbi^{32,55}, Miguel Tábuas-Pereira⁶⁶, Fabrizio Tagliavini²⁶, Mikel Tainta³¹, Ricardo Taipa⁶⁷, David Tang-Wai⁶⁸, David L Thomas⁶⁹, Paul Thompson⁷⁰, Carolyn Timberlake²⁷, Pietro Tiraboschi²⁶, Emily Todd²¹, Philip Van Damme⁷¹, Mathieu Vandenbulcke⁷², Ana Verdelho⁷³, Jorge Villanua⁷⁴, Jason Warren²¹, Carlo Wilke⁴⁰, Elisabeth Wlasich⁴¹, Miren Zulaica³⁶

List of GENFI consortium affiliations:

1. Instituto Ciencias Nucleares Aplicadas a Saude, Universidade de Coimbra, Coimbra, Portugal.
2. Faculty of Medicine, University of Coimbra, Coimbra, Portugal.
3. Department of Neurology, University of Ulm, Ulm, Germany.
4. Department of Clinical Neuroscience, Karolinska Institutet, Stockholm, Sweden.
5. Alzheimer's disease and Other Cognitive Disorders Unit, Neurology Service, Hospital Clínic, Barcelona, Spain.
6. Biotechnology Laboratory, Department of Diagnostics, ASST Brescia Hospital, Brescia, Italy.
7. Fondazione IRCCS Ca' Granda Ospedale Maggiore Policlinico, Neurodegenerative Diseases Unit, Milan, Italy; University of Milan, Centro Dino Ferrari, Milan, Italy.
8. Alzheimer's disease and Other Cognitive Disorders Unit, Neurology Service, Hospital Clínic, Barcelona, Spain.
9. Cognitive Disorders Unit, Department of Neurology, Donostia University Hospital, San Sebastian, Gipuzkoa, Spain; Neuroscience Area, Biodonostia Health Research Institute, San Sebastian, Gipuzkoa, Spain.
10. Imaging Diagnostic Center, Hospital Clínic, Barcelona, Spain.
11. Department of Medical Biophysics, The University of Western Ontario, London, Ontario, Canada; Centre for Functional and Metabolic Mapping, Robarts Research Institute, The University of Western Ontario, London, Ontario, Canada.
12. Department of Diagnostic and Interventional Neuroradiology, University of Tübingen, Tübingen, Germany.
13. Centre for Neurodegenerative Disorders, Department of Clinical and Experimental Sciences, University of Brescia, Italy.
14. Inserm 1172, Lille, France.
15. CHU, CNR-MAJ, Labex Distalz, LiCEND Lille, France.
16. Sorbonne Université, Paris Brain Institute – Institut du Cerveau – ICM, Inserm U1127, CNRS UMR 7225, AP-HP - Hôpital Pitié-Salpêtrière, Paris, France.
17. Centre pour l'Acquisition et le Traitement des Images, Institut du Cerveau et la Moelle, Paris, France.
18. Department of Neurology, Ludwig-Maximilians Universität München, Munich, Germany.
19. Department of Neuroscience, Psychology, Drug Research and Child Health, University of Florence, Florence, Italy.
20. Sunnybrook Health Sciences Centre, Sunnybrook Research Institute, University of Toronto, Toronto, Canada.
21. Dementia Research Centre, Department of Neurodegenerative Disease, UCL Institute of Neurology, Queen Square, London, UK.
22. Center for Neurodegenerative Science, Van Andel Institute, Grand Rapids, Michigan, MI 49503, USA.
23. Laboratory for Cognitive Neurology, Department of Neurosciences, KU Leuven, Leuven, Belgium.
24. Biomedical Research Institute, Hasselt University, 3500 Hasselt, Belgium.
25. CITA Alzheimer, San Sebastian, Gipuzkoa, Spain.
26. Fondazione IRCCS Istituto Neurologico Carlo Besta, Milano, Italy.
27. Department of Clinical Neuroscience, University of Cambridge, Cambridge, UK.

28. Univ Lille, France.
29. Inserm 1172, Lille, France.
30. CHU, CNR-MAJ, Labex Distalz, LiCEND Lille, France.
31. Neuroscience Area, Biodonostia Health Research Institute, San Sebastian, Gipuzkoa, Spain.
32. Department of Neuroscience, Psychology, Drug Research and Child Health, University of Florence, Florence, Italy.
33. Laboratory of Neurosciences, Institute of Molecular Medicine, Faculty of Medicine, University of Lisbon, Lisbon, Portugal.
34. Baycrest Health Sciences, Rotman Research Institute, University of Toronto, Toronto, Canada
35. Centre de référence des démences rares ou précoces, IM2A, Département de Neurologie, AP-HP - Hôpital Pitié-Salpêtrière, Paris, France
36. Neuroscience Area, Biodonostia Health Research Institute, San Sebastian, Gipuzkoa, Spain.
37. Neuroradiology Unit, University of Brescia, Brescia, Italy.
38. Alzheimer Disease Research Unit, McGill Centre for Studies in Aging, Department of Neurology & Neurosurgery, McGill University, Montreal, Québec, Canada.
39. Neurology, ASST Brescia Hospital, Brescia, Italy.
40. Department of Neurodegenerative Diseases, Hertie-Institute for Clinical Brain Research and Center of Neurology, University of Tübingen, Tübingen, Germany.
41. Neurologische Klinik, Ludwig-Maximilians-Universität München, Munich, Germany.
42. Division of Clinical Geriatrics, Karolinska Institutet, Stockholm, Sweden.
43. Department of Neurology, Erasmus Medical Center, Rotterdam, Netherlands.
44. The University Health Network, Toronto Rehabilitation Institute, Toronto, Canada.
45. Division of Neuroscience and Experimental Psychology, Wolfson Molecular Imaging Centre, University of Manchester, Manchester, UK.
46. Manchester Centre for Clinical Neurosciences, Department of Neurology, Salford Royal NHS Foundation Trust, Manchester, UK.
47. Département de Neurologie, AP-HP - Hôpital Pitié-Salpêtrière, Paris, France
48. Centre de Neurosciences and Cell Biology, Universidade de Coimbra, Coimbra, Portugal.
49. German Center for Neurodegenerative Diseases (DZNE), Munich, Germany.
50. Munich Cluster of Systems Neurology (SyNergy), Munich, Germany.
51. Neurologische Klinik, Ludwig-Maximilians-Universität München, Munich, Germany.
52. Laboratory of Language Research, Centro de Estudos Egas Moniz, Faculty of Medicine, University of Lisbon, Lisbon, Portugal.
53. MRC Prion Unit, Department of Neurodegenerative Disease, UCL Institute of Neurology, Queen Square, London, UK.
54. Department of Clinical Genetics, Erasmus Medical Center, Rotterdam, Netherlands.
55. IRCCS Fondazione Don Carlo Gnocchi, Florence, Italy.
56. Department of Medical Statistics, London School of Hygiene and Tropical Medicine, London, UK.
57. Center for Alzheimer Research, Division of Neurogeriatrics, Department of Neurobiology, Care Sciences and Society, Bioclinicum, Karolinska Institutet, Solna, Sweden.
58. Unit for Hereditary Dementias, Theme Aging, Karolinska University Hospital, Solna, Sweden.
59. Amsterdam University Medical Centre, Amsterdam VUmc, Amsterdam, Netherlands.
60. Department of Biomedical, Experimental and Clinical Sciences "Mario Serio", Nuclear Medicine Unit, University of Florence, Florence, Italy.
61. Stroke Unit, ASST Brescia Hospital, Brescia, Italy.
62. Tanz Centre for Research in Neurodegenerative Diseases, University of Toronto, Toronto, Canada
63. Translational Neuroimaging Laboratory, McGill Centre for Studies in Aging, McGill University, Montreal, Québec, Canada.
64. University Hospital of Coimbra (HUC), Neurology Service, Faculty of Medicine, University of Coimbra, Coimbra, Portugal; Center for Neuroscience and Cell Biology, Faculty of Medicine, University of Coimbra, Coimbra, Portugal.
65. Department of Clinical Neurological Sciences, University of Western Ontario, London, Ontario, Canada.
66. Neurology Department, Centro Hospitalar e Universitário de Coimbra, Coimbra, Portugal.
67. Neuropathology Unit and Department of Neurology, Centro Hospitalar do Porto - Hospital de Santo António, Oporto, Portugal.
68. The University Health Network, Krembil Research Institute, Toronto, Canada.
69. Neuroimaging Analysis Centre, Department of Brain Repair and Rehabilitation, UCL Institute of Neurology, Queen Square, London, UK.

70. Division of Neuroscience and Experimental Psychology, Wolfson Molecular Imaging Centre, University of Manchester, Manchester, UK.
71. Neurology Service, University Hospitals Leuven, Belgium; Laboratory for Neurobiology, VIB-KU Leuven Centre for Brain Research, Leuven, Belgium.
72. Geriatric Psychiatry Service, University Hospitals Leuven, Belgium; Neuropsychiatry, Department of Neurosciences, KU Leuven, Leuven, Belgium.
73. Department of Neurosciences and Mental Health, Centro Hospitalar Lisboa Norte - Hospital de Santa Maria & Faculty of Medicine, University of Lisbon, Lisbon, Portugal.
74. OSATEK, University of Donostia, San Sebastian, Gipuzkoa, Spain.

		Dementia Research Institute at UCL, Cruciform Building			
Program: C9ORF72		Standard Operating Procedure		Page 1 of 6	
Title:	Simoa Homebrew poly(GP) assay protocol				
Protocol Id:	mGP/GP57-60_HD-X	Protocol Version No.:	2		
Responsible Scientist:	Eszter Katona	Date last revised:	28/01/2022		
Approvers:	Adrian Isaacs and Amanda Heslegrave	Approval Date:	16/02/2022		

Contents:

Step	Content
Table 1	Reagents
Table 2	Consumables
Table 3	Reagent volumes
Table 4	Sample volumes
Table 5	Assay set-up
Table 6	Procedure 1 – Maintenance task before a run
Table 7	Procedure 2 – Running assay on the HD-X
Table 8	Procedure 3 – After run: Data extraction and post-run maintenance

Table 1: Reagents

	Reagent Name	Reagent Concentration	Reagent Source	Catalogue Number
1.	System Wash Buffer 1	1x	Quanterix	100486
2.	System Wash Buffer 2	1x	Quanterix	100487
3.	Bead Diluent	1x	Quanterix	100458
4.	SBG Diluent	1x	Quanterix	100376
5.	Homebrew Detector/Sample Diluent	1x	Quanterix	101359
6.	Sample Diluent A kit	1x	Quanterix	101575
7.	SBG Concentrate	dependent on lot#	Quanterix	103397
8.	RGP Reagent	1x	Quanterix	103159
9.	Homebrew Helper Beads	dependent on lot#	Quanterix	103208
10.	Homebrew Carboxylated Beads	dependent on lot#	Quanterix	103207
11.	Standard peptide (GST-GP32)	Two starting stocks: 15000, 1500 pg/ml	Custom made – Wave Life Sciences	N/A
12.	Capture antibody (mGP conjugated to carboxylated beads)	Depends on aliquot	Developmental Studies Hybridoma Bank, Target ALS Foundation	tALS 828.179
13.	Detector antibody (biotinylated GP57-60)	Depends on aliquot	Custom made	N/A



		Dementia Research Institute at UCL, Cruciform Building			
Program: C9ORF72		Standard Operating Procedure		Page 2 of 6	
Title:	Simoa Homebrew poly(GP) assay protocol				
Protocol Id:	mGP/GP57-60_HD-X	Protocol Version No.:	2		
Responsible Scientist:	Eszter Katona	Date last revised:	28/01/2022		
Approvers:	Adrian Isaacs and Amanda Heslegrave	Approval Date:	16/02/2022		

Table 2: Consumables

	Name	Source	Catalogue Number
1.	Conical Well Plates for HD-1/X	Quanterix	101457
2.	Conductive Tips for Simoa HD-1/X Analyzer	Quanterix	101726
3.	Simoa Cuvettes Bulk Pack (rev 2)	Quanterix	103346
4.	Simoa Discs (16)	Quanterix	100001
5.	Reagent Bottle Pack for Simoa HD-1/X Analyzer	Quanterix	102411
6.	Simoa HD-1 Sealing Oil	Quanterix	100206
7.	Alternative: Disc Kit for Simoa HD-1/X Analyzer (rev 2)	Quanterix	103347
8.	DynaMag-2 Magnet magnetic separator	Thermo Fisher Scientific	12321D

Table 3: Reagent volumes

Reagent	Working concentration	Diluent	Volume /measurement (µl)	Extra pipettor volume/measurement (µl)	Dead volume/reagent holder (µl)	Total volume for n number of measurements (µl)
Assay beads (mGP)	6 × 10 ⁶ beads/ml	Bead diluent	25 µl	10 µl	600 µl	n × (25 + 10) + 600
Helper beads	14 × 10 ⁶ beads/ml					
Detector antibody	0.3 µg/ml	Homebrew Detector/ Sample diluent	20 µl			n × (20 + 10) + 600
SBG	50 pM	SBG diluent	100 µl			n × (100 + 10) + 600
RGP	N/A	N/A	50 µl	n × (50 + 10) + 600		

Table 4: Sample volumes

Sample type	Working concentration	Diluent	Volume/ Measurement (µl)	Extra pipettor volume/measurement (µl)	Dead volume/well (µl)	Total volume/sample in duplicate measurements (µl)
CSF	1:2	Diluent A	100	10	30	2 × (100 + 10) + 30
Calibrator	200, 150, 100, 80, 50, 25, 10, 5, 1, 0 pg/ml		100	10		2 × (100 + 10) + 30



		Dementia Research Institute at UCL, Cruciform Building			
Program: C9ORF72		Standard Operating Procedure		Page 3 of 6	
Title:	Simoa Homebrew poly(GP) assay protocol				
Protocol Id:	mGP/GP57-60_HD-X	Protocol Version No.:	2		
Responsible Scientist:	Eszter Katona	Date last revised:	28/01/2022		
Approvers:	Adrian Isaacs and Amanda Heslegrave	Approval Date:	16/02/2022		

Table 5: Assay set-up



Dilutions and Steps	Dilution Description	Neat
		Steps
Incubation time	Step 1 (Beads, Sample, Detector)	47 x cadences (45s)
	Step 2 (SBG)	7 x cadences (45s)

Table 6: Procedure 1 – Maintenance task before a run



Step	Step Description
1.	<p>If the first run of the day:</p> <ol style="list-style-type: none"> Turn on the PC and switch on the instrument. Launch the SIMOA software and wait until the instrument initialises and the instrument status is 'Ready'. Fill a reagent bottle with System Wash Buffer 1. Place the reagent bottle to 'Position 3' in a rack. Go to 'Maintenance' tab and select 'Start of the day'. Click on 'Run task'. Push rack into position 4 in the instrument and click 'Next' on the maintenance tab. Wait for the run to finish and once it is done click 'Close' to close the maintenance tab. <i>Maintenance task takes ~ 20 min.</i> Remove the rack from the instrument. <i>If 4 hrs have passed between the start of the assay run and the 'Start of the day' maintenance task, the 'Idle Fluid Prime' task needs to be performed before assay run can be initiated.</i>
2.	<p>If not the first run of the day:</p> <ol style="list-style-type: none"> If > 4 hrs have passed since 'Start of the day' maintenance task or previous assay run, go to 'Maintenance' tab and select 'Idle Fluid Prime'. Click 'Run task' and wait until maintenance task finishes. <i>Takes ~ 10 min.</i> Once finished, click 'Close'.

Table 7: Procedure 2 – Running assay on the HD-X



Step	Step Description
1.	<p>Once the maintenance task is finished, set up Homebrew assay, if not already done so.</p> <ol style="list-style-type: none"> You can download Homebrew assay definition from Quanterix Customer support website. This can be imported in the instrument at 'Custom Assay/ Assay Overview'. To set up assay, go to 'Custom Assay' tab and select the name of the Homebrew assay. Define number washes, dilution, assay beads, detector antibody, SBG, and RGP according to the conditions given above in the 'Assay set up' table.

		Dementia Research Institute at UCL, Cruciform Building			
Program: C9ORF72		Standard Operating Procedure		Page 4 of 6	
Title:	Simoa Homebrew poly(GP) assay protocol				
Protocol Id:	mGP/GP57-60_HD-X	Protocol Version No.:	2		
Responsible Scientist:	Eszter Katona	Date last revised:	28/01/2022		
Approvers:	Adrian Isaacs and Amanda Heslegrave	Approval Date:	16/02/2022		

	d) Set up calibrator concentrations and definitions under 'Plexes' tab. If helper beads are used, set up helper plex with the same calibrator concentrations. Set appropriate definitions and make sure that results are set to be hidden.
2.	Put required volume of RGP to a shaker at 800 rpm either at 30°C for ≥30 minutes or 25°C for ≥1 hr.
3.	Preparation of the assay bead: <ul style="list-style-type: none"> a) Take out Bead Diluent on ice. b) Add 1 ml Bead Diluent to a 2ml Eppendorf tube. c) Add the required volume of Bead Diluent to a reagent bottle. d) Vortex assay beads at high speed for 30 sec and add required volume to the 2 ml Eppendorf tube with 1 ml Bead Diluent. e) If helper beads are used, perform the same procedure with the helper beads. Note, that both the assay and helper beads go into the same 2 ml Eppendorf tube containing the bead diluent. f) Vortex mix for 5 sec and spin down for 10 sec at 1000×g. g) Place the tube on a magnetic separator for 1 min. h) Aspirate Bead Diluent then remove the tube from the magnetic separator. i) Resuspend beads in 1 ml Bead Diluent from the reagent bottle, then vortex beads for 5 sec and spin it down briefly to make sure that all liquid is removed from the cap. j) Add suspension to the reagent bottle. Pipette up and down twice to make sure all beads are added. k) Close reagent bottle, label with Homebrew Bead barcode, and place on a rotator to keep beads in solution while the rest of the reagents are being prepared.
4.	Preparation of the detector antibody: <ul style="list-style-type: none"> a) Take out Homebrew Detector/Sample Diluent and detector antibody stock on ice. b) Add the required volume of Homebrew Detector/Sample Diluent for detector antibody dilution to a reagent holder. c) Flick detector antibody stock tube to mix. Add the required volume of stock detector antibody to the diluent in the reagent holder. d) Close reagent holder, label with Homebrew Detector barcode, and place on a rotator while preparing the rest of the reagents.
5.	Preparation of SBG: <ul style="list-style-type: none"> a) Take out SBG diluent and SBG concentrate on ice. b) Add the required volume of SBG diluent to a reagent holder. c) Vortex SBG concentrate and add required volume to the diluent in the reagent holder to achieve 50 pM working concentration. d) Close the reagent holder, label with Homebrew SBG barcode, and put on a rotator to mix.
6.	Preparation of the calibrators: <ul style="list-style-type: none"> a) Take out Diluent A on ice. b) Take out standard stock to ice, briefly vortex, and spin down. c) Make up calibrator curve from peptide stock by serial dilution in Eppendorf tubes. Between each dilution, vortex dilution for 15 sec then briefly spin it down. Calibrator concentrations 200, 150, 100, 80, and 50 pg/ml are made up from the 15000 pg/ml stock while 25, 10, 5, 1, and 0 pg/ml are made up from the 1500 pg/ml stock. d) Place ready calibrators on ice.


		Dementia Research Institute at UCL, Cruciform Building			
Program: C9ORF72		Standard Operating Procedure		Page 5 of 6	
Title:	Simoa Homebrew poly(GP) assay protocol				
Protocol Id:	mGP/GP57-60_HD-X	Protocol Version No.:	2		
Responsible Scientist:	Eszter Katona	Date last revised:	28/01/2022		
Approvers:	Adrian Isaacs and Amanda Heslegrave	Approval Date:	16/02/2022		

	<i>The vial of calibrator stock in PCR tube is for a single use only so discard after use.</i>
7.	<p>Preparation of the samples:</p> <ol style="list-style-type: none"> Take out samples to thaw on ice. While samples are thawing, add the required volume of Diluent A to Eppendorf tubes. Place them on ice. Once samples thaw, vortex each for 15 sec, spin down briefly, and add the required volume to the already prepared diluent on ice to make up a 1:2 dilution. Repeat this for each of the samples. Place ready samples on ice.
8.	<p>Loading samples/calibrators on the plate:</p> <ol style="list-style-type: none"> Vortex each sample/calibrator for 15 sec and briefly spin down before loading on the plate. To avoid bubbles, use reverse pipetting when loading the samples. Make sure there are no bubbles in the samples because that would hinder the measurement. Duplicates are loaded onto the same well.
9.	<p>Loading reagents in the instrument:</p> <ol style="list-style-type: none"> Go to 'Load Reagent' tab and select a reagent lane. Beads: Vortex beads for 30 sec before loading. Scan the barcode of the beads and add available volume in the instrument. Load reagent bottle to one of the three shaking positions in the rack. <i>These are positions 1-3. Do not let beads sit for idle >5 min. If this happens, vortex again.</i> Detector: Scan the barcode of the detector and add available volume in software. Load reagent bottle in the rack. SBG: Scan the barcode of SBG and add available volume in software. Load the reagent bottle in the rack. Once all bead, detector, and SBG are loaded in the reagent rack, push the reagent rack in the appropriate lane in the instrument. RGP: Select an RGP lane. Scan the barcode of the RGP reagent. Take off the cap and load in the reagent rack. Load the reagent rack in the appropriate lane. <i>The vial of RGP is for single-day use only. Please discard any remaining at the end of the day.</i> Click 'Done Loading Reagents'.
10.	<p>Creating plate outline and loading plate in the instrument:</p> <ol style="list-style-type: none"> Go to 'Setup Run' tab. Assign a batch name (a run name) and assign plate barcode (plate can either be scanned or just be a random number for homebrew assays). Click 'Enter'. Assign calibrators: Select 'Assign calibrators' tab. Select a single well and assign the appropriate Homebrew assay. Select the highest calibrator (Calibrator A) and then click 'Descending'. This will assign the rest of the calibrators to the wells below. Set the appropriate number of replicates per well (here: duplicates). Assign samples: Select 'Assign samples' tab. Select all the wells that contain samples. Assign the appropriate assay. Set the appropriate number of replicates per well (here: duplicates). Set dilution of samples to 'neat'. Place the plate on the plate rack and insert it to the appropriate lane. Touch 'Done with set up'.
11.	Check system resources. If required fill System Wash buffer 1, System Wash buffer 2, System liquid or load cuvettes, pipettes tips, or discs. If required, empty solid waste or liquid waste.

		Dementia Research Institute at UCL, Cruciform Building			
Program: C9ORF72		Standard Operating Procedure		Page 6 of 6	
Title:	Simoa Homebrew poly(GP) assay protocol				
Protocol Id:	mGP/GP57-60_HD-X	Protocol Version No.:	2		
Responsible Scientist:	Eszter Katona	Date last revised:	28/01/2022		
Approvers:	Adrian Isaacs and Amanda Heslegrave	Approval Date:	16/02/2022		

12.	If system resources are met, click 'Start run' in 'System resources' tab. If button is not active, check for further flags in 'Resource details' tab.
13.	If the run was started, go to 'Current run' tab to monitor assay run.

Table 8: Procedure 3 – After run: Data extraction and post-run maintenance

Step	Step Description
1.	Once the run is finished and the instrument is 'Ready', you can proceed with data extraction.
2.	<p><u>CSV file extraction:</u></p> <ol style="list-style-type: none"> Go to 'History and Reports' and click on 'Run history' tab. Filter results based on 'Batch ID'. Click 'Select all results' and then 'Export'. Select the location where you want to save it, name the file, and press 'Enter'. <p><u>Batch calibration report extraction:</u></p> <ol style="list-style-type: none"> Go to 'History and Reports' and click on 'Reports' tab. Select 'Batch calibration report' and select the appropriate batch (run name). Click on 'Preview' and once the report is in preview, click on 'Export'. Select the appropriate location where files need to be saved, name the file and press enter to export batch calibration report as a pdf. Select 'Done' to close the tab. <p><i>Further data can be extracted, or values can be recalculated. Refer to Homebrew Assay Development Guide from Quanterix.</i></p>
3.	Remove the racks from the instrument and discard reagent bottles, RGP, and plates.
4.	Run 'End of the day' maintenance task for post-run maintenance. Load a reagent bottle with System wash buffer 1 and load it into position 3 in a reagent rack.
5.	Go to 'Maintenance' tab, select 'End of the day' maintenance task, and click 'Run task'.
6.	Push the reagent rack to lane 4 and click 'Next' in 'Maintenance' tab. <i>Wait until the maintenance task is finished, ~15 min.</i>
7.	Once 'End of the day' maintenance task finished, the instrument can be switched off.
8.	<p>Switching off:</p> <ol style="list-style-type: none"> Shutdown software by clicking on  and select 'Shut down'. This will close the software. Shut down the computer then switch off the instrument.